

Deciduous dentition and dental eruption of Hyainailouroidea (Hyaenodonta, “Creodonta,” Placentalia, Mammalia)

Matthew R. Borths and Nancy J. Stevens

ABSTRACT

Deciduous dental morphology and the sequence of permanent dental eruption offer developmental and phylogenetic insights into mammalian evolution. Early life history in Hyaenodonta, a morphologically diverse and biogeographically widespread clade of carnivorous mammals known from the Paleogene and early Neogene, has only been examined closely in one genus: *Hyaenodon*. Here we describe the deciduous dental morphology for six hyainailouroids, a clade of hyaenodonts distantly related to *Hyaenodon* that dominated early Cenozoic meat-eating niches of Afro-Arabia for nearly 20 Ma. Results suggest significant variation among hyainailouroids in expression of the dP³ and dP⁴ protocone, paracone, and metacone and in expression of the dP₃ and dP₄ paraconid, metaconid, and talonid. Deciduous dental characters were incorporated into a Bayesian phylogenetic analysis. The topology was congruent with earlier systematic examinations of hyaenodont evolution, suggesting that deciduous dental features can be phylogenetically informative and that taxa known only from deciduous teeth can be incorporated into studies of mammalian systematics. Based on the specimens described herein, the dental eruption sequence of Hyainailouroidea is reconstructed. P⁴ and P³ erupt after M³, evidence that the deciduous carnassial complex formed between dP³ and dP₄ was retained until late in development, permitting hyaenodonts to heavily wear shearing blades on these teeth before replacement. This differs from Carnivora, a group that tends to replace deciduous dentition earlier in development, effectively limiting carnivorans to a single set of carnassials throughout most of their lifespan. This developmental difference between carnivorans and hyaenodonts can now be examined in a larger systematic and ecological context.

Matthew R. Borths. Department of Biomedical Sciences, Heritage College of Osteopathic Medicine, Ohio University, Athens, Ohio 45701, USA; Center for Ecology and Evolutionary Studies, Ohio University, Athens, Ohio 45701, USA. borths.1@gmail.com

Nancy J. Stevens. Department of Biomedical Sciences, Heritage College of Osteopathic Medicine, Ohio University, Athens, Ohio 45701, USA; Center for Ecology and Evolutionary Studies, Ohio University, Athens, Ohio 45701, USA. stevensn@ohio.edu

Borths, Matthew R. and Stevens, Nancy J. 2017. Deciduous dentition and dental eruption of Hyainailouroidea (Hyaenodonta, “Creodonta,” Placentalia, Mammalia). *Palaeontologia Electronica* 20.3.55A: 1-34. <https://doi.org/10.26879/776>
palaeo-electronica.org/content/2017/2056-deciduous-hyaenodont-teeth

Copyright: November 2017 Society for Vertebrate Paleontology.

This is an open access article distributed under the terms of Attribution-NonCommercial-ShareAlike 4.0 International (CC BY-NC-SA 4.0), which permits users to copy and redistribute the material in any medium or format, provided it is not used for commercial purposes and the original author and source are credited, with indications if any changes are made.
creativecommons.org/licenses/by-nc-sa/4.0/

Keywords: Ontogeny; Carnivory; Egypt; Africa; Paleogene

Submission: 26 April 2017 Acceptance: 31 October 2017

INTRODUCTION

Fossilized remains of animals are often interpreted by paleontologists as phenotypes shaped by natural selection (e.g., Stern and Susman, 1983; Shubin et al., 2006; Tseng et al., 2016), with hypotheses surrounding adaptation, niche occupation, evolution, and extinction of a species typically examined through the lens of the adult phenotype (e.g., Ross, 1996; Finarelli and Flynn, 2009; Goswami and Polly, 2010). Yet examination of extant organisms demonstrates that natural selection acts throughout the life cycle, and fitness is significantly impacted by developmental stages that precede maturity (Lindström, 1999). Hence the adaptive strategies employed by a species or lineage can only truly be understood through deeper knowledge of the ontogeny of a species or lineage (Sánchez-Villagra, 2010a; Codron et al., 2013; Urdy et al., 2013; Hone et al., 2016). As a heritable aspect of an animal's biology, developmental data is also a rich source of phylogenetic information, providing insight into evolutionary relationships (e.g., de Queiroz, 1985; Smith, 2000; Asher and Lehmann, 2008).

In mammals, the reduction of dental replacement to diphyodonty has built a readily preserved ontogenetic calibration point into the mouths of most taxa (Anders et al., 2011). The replacement of deciduous teeth, eruption of adult dentition, and subsequent wear contribute information on the rate of maturation across lineages (e.g., Slaughter et al., 1974, Smith, 2000; Asher and Lehmann, 2008; Ciancio et al., 2012; Veitschegger and Sánchez-Villagra, 2016). Dental eruption sequences can be compared with other proxies for developmental maturity, such as long bone epiphyseal fusion (Coutinho et al., 1993; Uhen, 2000) and cranial suture fusion (Sánchez-Villagra, 2010b; Rager et al., 2013), to identify key developmental phases in extinct taxa that can be used to reconstruct life histories and phylogenetic relationships (Fink, 1982; Smith, 1989; O'Leary et al., 2013).

Hyaenodonta is a diverse radiation of carnivorous placental mammals found in terrestrial ecosystems in Eurasia, North America, and Afro-Arabia throughout the Paleogene (Rose, 2006). The clade persisted into the Neogene in Asia and

Afro-Arabia, making it the longest-lived radiation of meat-eating placental mammals besides Carnivora (Lewis and Morlo, 2010). Parsing out the evolution, life history, and extinction of Hyaenodonta is critical for building a larger understanding of the evolution of the niches occupied by modern carnivorous mammals. Previous work on the dental development of hyaenodonts focused on the genus *Hyaenodon*, a genus from the Eurasian and North American clade Hyaenodontinae (Mellet, 1977; Bastl et al., 2011; Bastl and Nagel, 2013; Bastl et al., 2014); deciduous dental materials preserved in other hyaenodonts (e.g., *Lesmesodon*, *Cynohyaenodon*, *Paroxyaena*) have received somewhat less attention (but see Morlo and Habersetzer, 1999; Lavrov, 2007). Recent systematic research demonstrates that *Hyaenodon* is only distantly related to Hyainailouroidea, a separate hyaenodont clade that contains hypercarnivorous taxa and all Afro-Arabian hyaenodonts (Rana et al., 2015; Borths et al., 2016). But only a few deciduous teeth have been described from Afro-Arabian hyaenodonts (Morales et al., 2010; Solé et al., 2016), making it difficult to compare the life histories of Afro-Arabian hyainailouroids to Eurasian and North American hyaenodont lineages and to use deciduous dental morphology and dental eruption to probe phylogenetic relationships among key taxa in this important group of early Cenozoic predators.

In this study, we describe and refer hyaenodont deciduous dental specimens from the late Eocene-early Oligocene (Fayum Depression, Egypt) and the early Miocene (Rusinga Island and Fort Ternan, Kenya) to five known hyainailouroid genera: *Apterodon*, *Leakitherium*, *Anasinopa*, *Disopsalis*, *Masrasector*, and *Metasinopa*. We compare the new deciduous dental material to Eurasian and North American hyaenodont materials to reconstruct dental development patterns among hyainailouroids. Building upon the efforts of Bastl et al. (2014), we incorporate this new morphological information into a phylogenetic analysis that includes deciduous dental characters. Finally, we use morphological and developmental data preserved in these specimens to discuss how hyaenodont dental development informs our understanding of life history strategies in the clade.

MATERIALS AND DESCRIPTIVE METHODS

Permissions

Specimens bearing DPC reference numbers described herein are available at the Division of Fossil Primates at the Duke Primate Center in Raleigh, NC and were collected and exported with permission granted by the Egyptian Mineral Resources Authority (formerly the Egyptian Geological Survey and Mining Authority) and the Egyptian Geological Museum. Specimens bearing KNM reference numbers described herein are available at the Nairobi National Museum, part of the National Museums of Kenya, and were examined under research permits issued by the Kenyan National Commission for Science, Technology and Innovation and as research affiliates of the National Museums of Kenya.

Institutional Abbreviations

BMNH, Natural History Museum, London; DPC, Duke Lemur Center, Division of Fossil Primates, Duke University, Durham, NC; KNM, National Museums of Kenya, Nairobi.

Morphological Measurements and Nomenclature

Dental measurements were collected from digital photographs of the specimens using ImageJ (Schneider et al., 2012). Dental nomenclature and measurement definitions follow Borths et al. (2016) and Holroyd (1999).

CT Scanning and Rendering

The μ -CT scans of DPC specimens were collected at the Duke University Shared Materials Instrumentation Facility using a Nikon XTH 225 ST scanner following the protocol described in Miller et al. (2017). Surface models and figures illustrating developing dentition were constructed using Avizo 7.0. Digital models of all scanned specimens are available at Morphosource (Project P393) (www.morphosource.org).

SYSTEMATIC PALEONTOLOGY

Class MAMMALIA Linnaeus, 1758
 Order HYAENODONTA Van Valen, 1967 sensu Solé et al., 2015
 Superfamily HYAINAILOUROIDEA Borths, Holroyd, and Seiffert, 2016
 Subfamily APTERODONTINAE Szalay, 1967
 Genus APTERODON Fischer, 1880

Type species. *Apterodon gaudryi* Fischer, 1880.

Other included species. *Apterodon altidens* Schlosser, 1910; *Apterodon intermedius* Lange-Badré and Böhme, 2005; *Apterodon langebadrae* Grohé et al., 2012; *Apterodon macrognathus* Andrews, 1904; *Apterodon saghensis* Simons and Gingerich, 1974.

Apterodon macrognathus Andrews, 1904
 Figures 1-2, Tables 1-2

Referred specimens. DPC 4126, right maxilla fragment with dP⁴ (Fayum Depression, Jebel Qatrani Formation, Quarry M); DPC 8217, left dentary fragment with dP₃, dP₄, M₁ (Fayum Depression, Jebel Qatrani Formation, Quarry M). Note: These specimens were not found in association.

Description

In the maxilla of *Apterodon macrognathus* (DPC 4126; Figure 1) the infraorbital foramen is superior and slightly anterior to the mesial root of dP⁴. The parastyle is mesiodistally short and divided by a buccolingually compressed ridge that continues the preparacrista onto the parastyle. The tall paracone is crenulated and buccolingually compressed and rises to an acute, slightly distally-directed peak. The metacone is individuated from the paracone and rises over half the height of the paracone after the cusps diverge. The mesiodistal length of the paracone base is subequal to the mesiodistal length of the metacone. The metacone forms a distinct carnassial notch with the buccolingually compressed and mesiodistally short metastyle. The metastyle rises to a distinct apex that is approximately one-third the height of the metacone. The buccal margin of the tooth is traced by a distinct, beaded buccal cingulum that connects the parastyle to the metastyle, dipping ventrally at the distobuccal face of the paracone. The protocone is mesiodistally broad. The lingual point of the protocone is a distinct cusp that projects to the same height as the apex of the metastyle. The trigon basin is deep and defined by a wide lingual cingulum. The alveoli of dP³ are also preserved, indicating the root that supported the protocone of dP³ was closely packed with the distal root of dP³.

In the dentary of *Apterodon macrognathus* (DPC 8217, Figure 2) dP₃ is a buccolingually compressed tooth with a prominent protoconid and small, but distinct talonid. The preprotocristid curves distally to the apex of the protoconid. The postprotocristid slopes more gently to the cristid obliqua. The entoconid is a prominent, sectorial cusp along the buccal margin of the talonid. Distinct buccal and lingual cingula rim the entire dou-

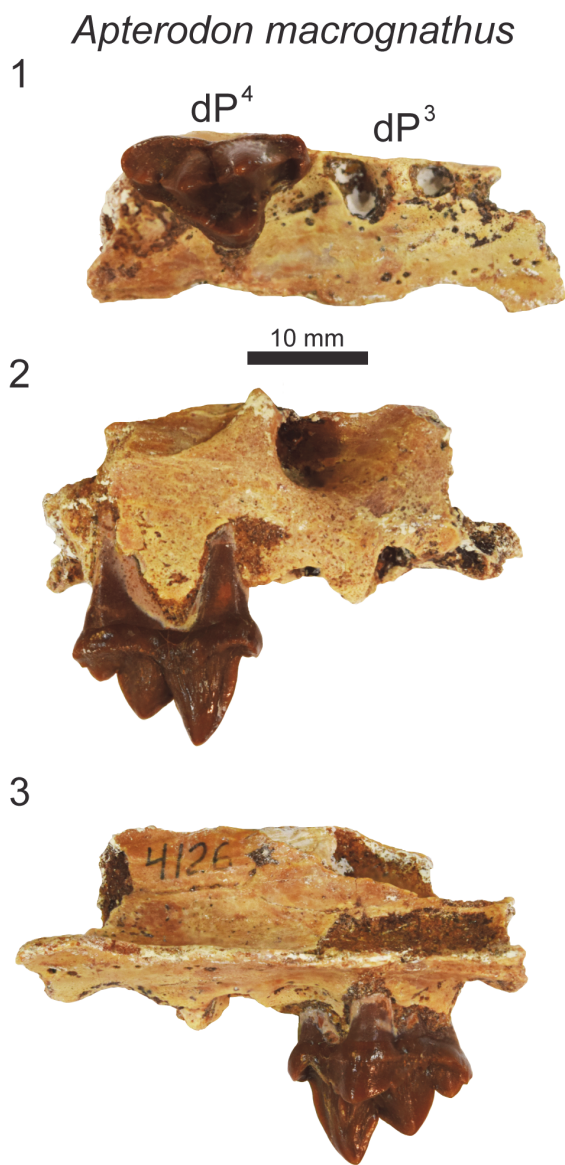


FIGURE 1. *Apterodon macrognathus* left maxilla fragment with dP⁴ and alveoli of dP³ (DPC 4126) from Quarry M (early Oligocene) in the Fayum Depression, Egypt in **1**) occlusal view; **2**) buccal view; and **3**) lingual view. Scale bar is 10 mm.

ble-rooted tooth. A mesiodistally elongate protoconid dominates the outline of dP⁴. The paraconid is low and mesiodistally short. The carnassial notch dives to the same level as the cristid obliqua. As on dP₃, the protoconid points slightly distally. The pre- and postprotocristid are buccolingually compressed and blade-like. The postprotocristid forms a deep notch at the cristid obliqua. The entoconid rises from the notch to a point taller than the paraconid and nearly half the height of the protoconid. There is no indication of a metaconid on

dP₄. The μ -CT of the dentary of *Apterodon macrognathus* (Figure 2) indicates the protoconid of M₂ was formed before the germs of either P₄ or P₃ began to coalesce.

Remarks

Apterodontines combine a key morphological feature of hypercarnivores, the reduction or absence of metaconids on the lower molars, with features of more generalist carnivores such as well-developed talonids on the lower molars, divergent metacones and paracones, and mesiodistally abbreviated metastyles on the upper molars (Van Valkenburgh, 2007) complicating dietary and phylogenetic inferences (Van Valen 1966; Szalay, 1967; Grohé et al., 2012). Recent phylogenetic studies (Borths et al., 2016; Borths and Seiffert, 2017) incorporate morphological features of the cranial vault (Solé et al., 2015), suggesting Apterodontinae as the sister clade of Hyainailourinae. Like the hyainailourines *Paroxyaena* and *Leakitherium*, the dP⁴ of *Apterodon macrognathus* (Figure 1) exhibits a buccolingually compressed paracone that is distally directed. *A. macrognathus* also shares with *Leakitherium* and *Paroxyaena* a mesiodistally short metastyle on dP⁴, crenulated enamel, and a lobe-like protocone. In contrast, the dP⁴ of the teratodontines *Metasinopa* and *Masractor* exhibit extensive metastyles, smooth and thin enamel, and buccolingually narrow protocones, morphology shared with *Pakakali*, a hyaenodont from the late Oligocene of the Rukwa Rift Basin (Borths and Stevens, 2017). These observations, in conjunction with the phylogenetic analysis conducted here to test the utility of deciduous dental characters, support the close relationship between Apterodontines and Hyainailouridae.

Family HYAINAILOURIDAE Pilgrim, 1932 sensu
Borths et al., 2016

Subfamily HYAINAILOURINAE Pilgrim, 1932

Genus LEAKITHERIUM Savage, 1965

Type and only species. *Leakitherium hiwegi* Savage, 1965.

Leakitherium hiwegi Savage, 1965

Figure 3, Tables 1-2

Referred specimens. KNM-RU 2949, left maxilla fragment with dP³ and dP⁴ (CMF 4025 in Savage, 1965; Rusinga Island, Kenya); KNM-RU 15182, maxilla fragment with dP³, dP⁴, P⁴ in crypt (Rusinga Island, Kenya).

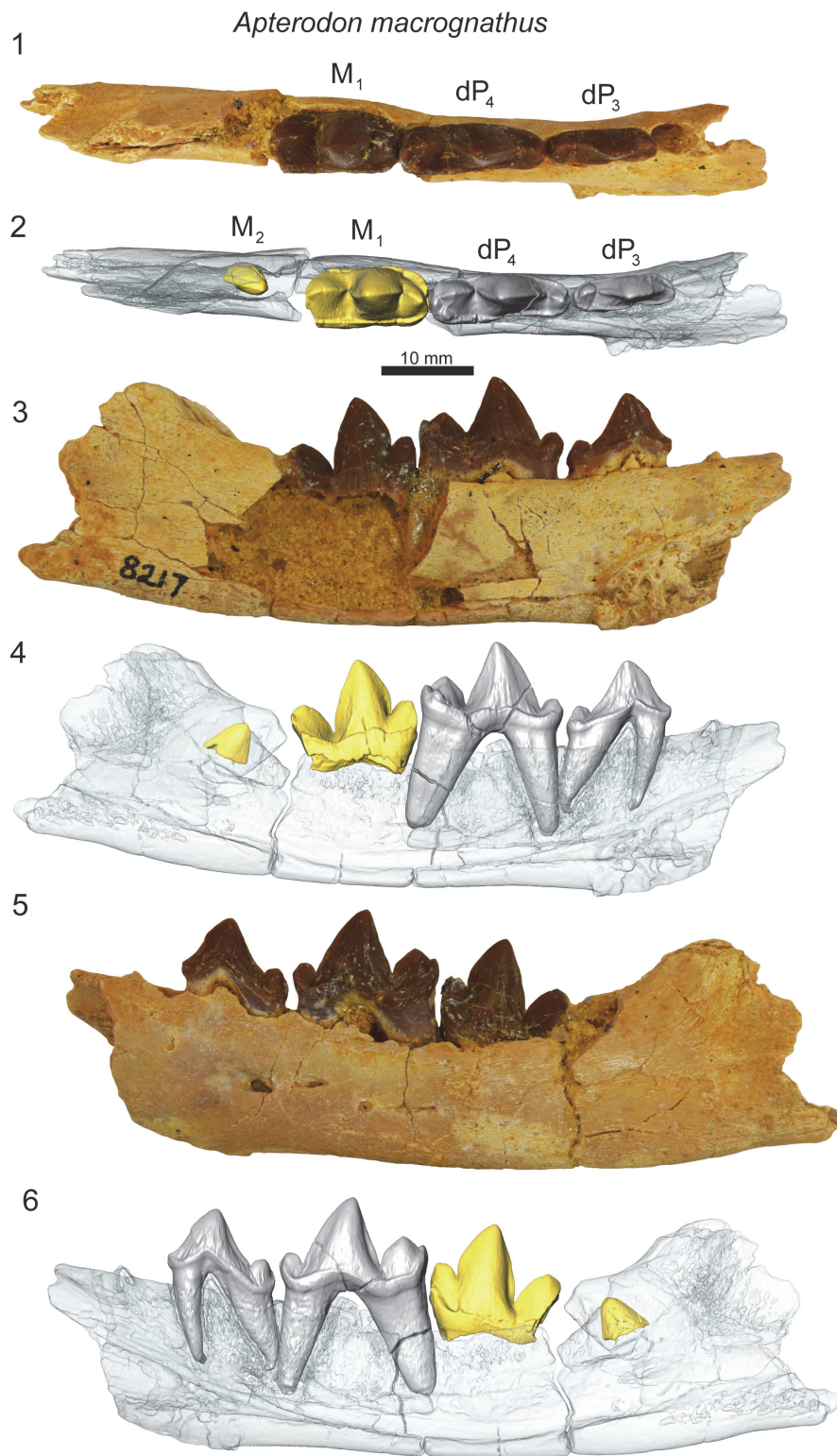


FIGURE 2. *Apterodon macrognathus* left dentary with dP₃, dP₄, M₁ and M₂ in crypt (DPC 8217) from Quarry M (early Oligocene) in the Fayum Depression, Egypt. Original specimen figured with digital model based on μ -CT scans reconstructed in Avizo. Mandibular corpus rendered transparent to reveal developing dentition. Grey, deciduous dentition. Yellow, permanent dentition. **1)** Specimen occlusal view; **2)** model occlusal view; **3)** specimen lingual view; **4)** model lingual view; **5)** specimen buccal view; **6)** model buccal view. Scale bar is 10 mm.

TABLE 1. Measurements of the upper dentition. Asterisk indicates the measurements are based on the alveoli of the tooth. Length is mesiodistal length. Width is buccolingual length. ~, indicates an approximate measurement based on fragmentary material. See methods for definitions of these measurements.

Taxon	Specimen	Tooth	Length	Width
<i>Apterodon macrognathus</i>	DPC 4126	dP3*	10.8	4.9
		dP4	15.6	9.0
<i>Leakitherium hiwegi</i>	KNM-RU 2949	dP3	15.4	10.8
		dP4	16.7	13.4
<i>Leakitherium hiwegi</i>	KNM-RU 15182	dP3	15.2	14.0
		dP4	~16.5	17.5
<i>Anasinopa leakeyi</i>	KNM-RU 2385	dP2	9.0	3.7
		dP3	9.6	6.7
		dP4	10.2	9.2
<i>Dissopsalis pyroclasticus</i>	KNM-FT 3357	dP3	15.4	9.2
		dP4	15.6	13.4
		M1*	15.5	16.0
<i>Masrasector nananubis</i>	DPC 20882	dP3	4.8	~3.0
		dP4	4.4	2.7
<i>Masrasector nananubis</i>	DPC 13837	dP3	5.0	3.0
		dP4	5.0	3.4
		M1	5.7	4.5
<i>Metasinopa</i> sp.	DPC 10199	dP3	10.5	5.1
		dP4	10.9	7.1
		M1	12.5	11.7

Description

KNM-RU 2949, a maxilla fragment of *Leakitherium hiwegi* (Figure 3), preserves the crowns of both dP³ and dP⁴. This specimen was originally numbered CMF 4025 and was briefly described and illustrated by Savage (1965) as P⁴ and M¹ and designated as the paratype of *Leakitherium*. Though the infraorbital foramen is not preserved intact, the floor of the infraorbital canal traces to a point superior to the mesial root of dP³. The parastyle of dP³ is relatively short compared to the mesiodistally elongate metastyle. The paracone and metacone are fused at the base and for most of the height of the metacone. The apex of the metacone is distinct from the paracone, but it is a smaller, mesiodistally shorter cusp. The postmetacrista slopes to the deep carnassial notch formed with the metastyle. No buccal cingulum is observed along the buccal margin of the tooth, though it should be noted the specimens are heavily abraded. A thin, lingual cingulum traces the low and mesiodistally wide protocone. The primary

cusps of the protocone rises only to the height of the parastyle.

The dP³ contacts dP⁴ lingual to the relatively small dP⁴ parastyle. The parastyle exhibits a small cusp that connects to the preparacrista. The paracone and metacone are fused for most of their height. The paracone is slightly taller than the lower, more buccolingually compressed metacone. The postmetacrista forms a distinct carnassial notch with the metastyle. The metastylar blade exhibits a slight undulation. The protocone of dP⁴ is mesiodistally narrower and projects more mesially than does the protocone of dP³. The distinct protocone cusp frames a shallow and clearly delineated trigon basin. The protocone on dP⁴ is low and does not rise to the level of the parastyle on dP⁴. The palate between the protocones of dP³ and dP⁴ and distal to the protocone of dP⁴ is deeply embayed, presumably to accommodate tall trigonids on dP₄ and M₁.

A second maxilla fragment of *Leakitherium*, KNM-RU 15182 (Figure 3), also preserves dP³ and dP⁴. Both crowns are fragmented or worn, though

TABLE 2. Measurements of the lower dentition. Asterisk indicates the measurements are based on the alveoli of the tooth. Length is mesiodistal length. Width is buccolingual length. ~, indicates an approximate measurement based on fragmentary material. See methods for definitions of these measurements.

Taxon	Specimen	Tooth	Length	Width
<i>Apterodon macrognathus</i>	DPC 8217	dP ₃	11.7	3.8
		dP ₄	15.7	4.9
		M ₁	14.0	6.5
<i>Anasinopa libyca</i>	BMNH M82378	dP ₃	9.9	2.2
		dP ₄	11.7	3.6
<i>Masrasector nananubis</i>	DPC 10358	dP ₃	5.2	1.6
		dP ₄	5.0	2.2
		M ₁	4.7	2.6
		M ₂	5.6	3.3
<i>Masrasector nananubis</i>	DPC 18276	dP ₂	3.9	1.5
		dP ₃	5.1	1.6
		dP ₄	4.7	1.8
<i>Metasinopa</i> sp.	DPC 4544	P ₂	9.2	2.4
		dP ₃ *	12.0	2.6
		dP ₄ *	10.4	3.0
		M ₁	10.6	4.7
		M ₂	12.6	5.2
		M ₃	~13.82	4.3

the morphology of the bases of each is consistent with the morphology observed on KNM-RU 2949, including the emergence of the infraorbital canal superior to the mesial root of dP₃. KNM-RU 15182 also preserves the enamel bell of P₄ in the crypt superior to the roots of dP₄. The developing tooth bears the distinctive crenulated enamel often associated with *Leakitherium* (Savage, 1965; Lewis and Morlo, 2010). There is no developing tooth apparent in the crypt superior to dP₃. This may be evidence that P₄ developed and erupted before P₃ in *Leakitherium*. It is also possible that the germ of P₃ was more developed than P₄ and fell out of the specimen when it was fractured along the P₃ crypt.

Remarks

The holotype of *Leakitherium* (BMNH M19083) is a pair of molars, M₁ and M₂, which both exhibit large protocones and expansive trigon basins (Savage, 1965). The lower dentition of *Leakitherium* has not been described. Some authors (Van Valen, 1967; Morales et al., 2007) have suggested *Leakitherium hiwegi* is the upper dentition of *Isohyaenodon andrewsi*. Holroyd (1999) made the case that the *Metapterodon kai-*

seri (known from upper dentition) and *Isohyaenodon andrewsi* (known from lower dentition) are in fact synonymous, and *Leakitherium* is a distinct taxon. Neither *Isohyaenodon andrewsi*, nor *Metapterodon kaiseri* exhibit the distinct, crenulated enamel of *Leakitherium*. Further, *Isohyaenodon* does not possess distinct talonids nor the buccolingually broad trigonids expected to occlude with the M₁ and M₂ of *Leakitherium*. The specimens referred to *Leakitherium* in this study share the crenulated enamel and buccolingual breadth noted in the M₁ and M₂ of the holotype (Savage, 1965). The rugosity of the enamel is even more pronounced on the unerupted P₄ (KNM-RU 15182, Figure 3), than on the more worn and abraded dP₄. Based on these observations, we support the hypothesis of Holroyd (1999) that *Leakitherium* is a distinct taxon.

The Borths et al. (2016) analysis places *Leakitherium* within Hyainailourinae, a result congruent with earlier phylogenetic hypotheses (Lewis and Morlo, 2010). One feature uniting hyainailourines is the metacone morphology on M₁ and M₂, reduced into a buccolingually compressed cusp that is partially or almost entirely fused to the paracone

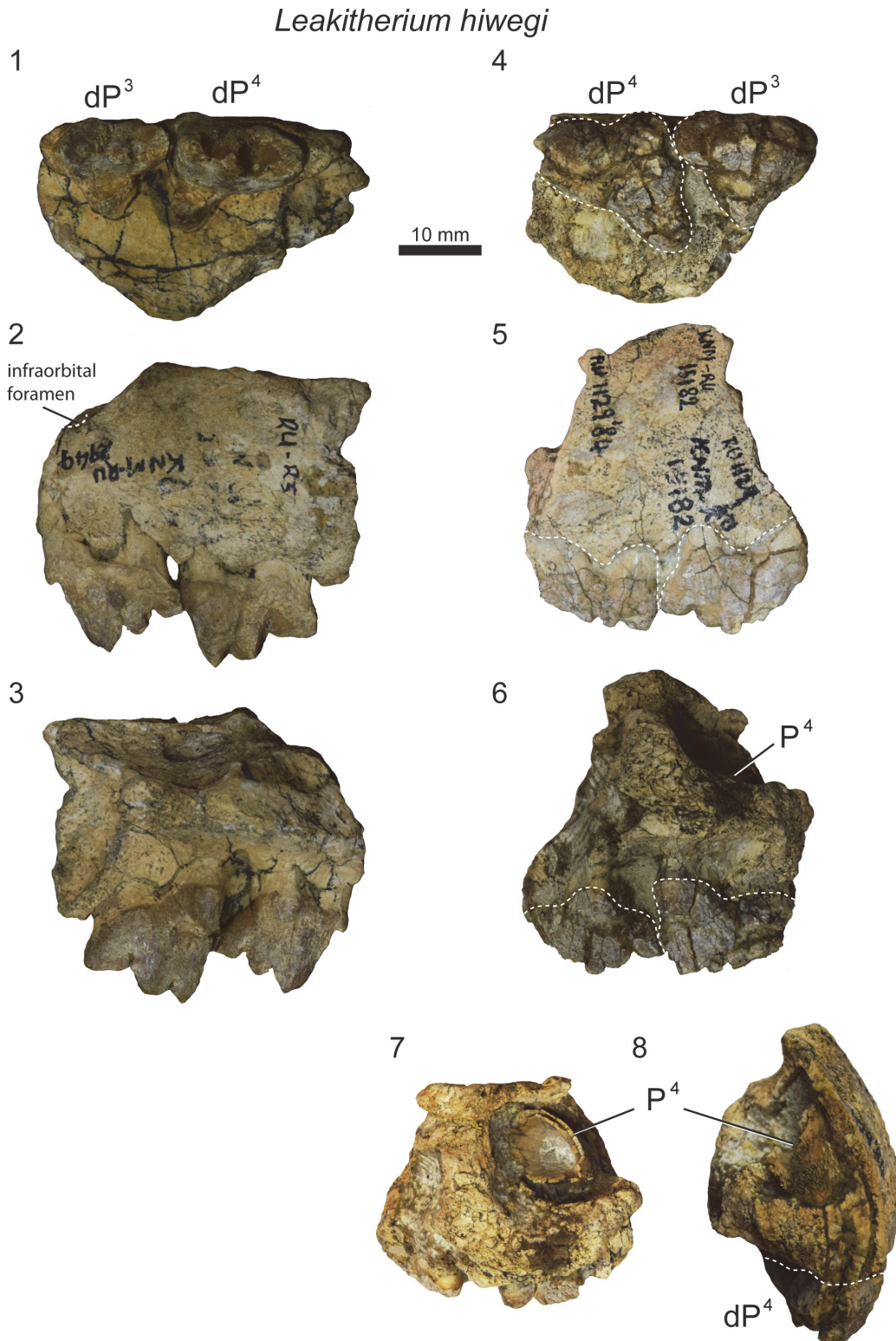


FIGURE 3. *Leakitherium hiwegi* maxilla fragments from Rusinga Island (early Miocene), Kenya. KNM-RU 2949 (CMF 4025 in Savage, 1965) is a left maxilla fragment dP³ and dP⁴ shown in **1**) occlusal view; **2**) buccal view; and **3**) lingual view. KNM-RU 15182 is a right maxilla fragment with dP³ and dP⁴ and the germ of P⁴ shown in **4**) occlusal view; **5**) buccal view; **6**) lingual view; **7**) dorsal view; **8**) and distal view. The well-developed germ of P⁴ is best viewed in dorsal and distal view. Specimens are to scale and scale bar is 10 mm.

(Borths et al., 2016). Interestingly, the dP⁴ of *Leakitherium* (Figure 3) exhibits a distinct metacone that is lower than and partially fused to the paracone, anticipating the morphology of M¹ in the holotype of *Leakitherium*. Indeed, the morphology the dP⁴ metacone in *Leakitherium* is similar to the dP⁴ metacone of *Paroxyaena pavlovi*, a smaller hyainailourine from the late Eocene of France (Lavrov, 2007). This reflects the observation that in many mammals, a deciduous tooth resembles the adult tooth in the immediately distal position (Zack, 2012).

Deciduous teeth also provide additional features useful in differentiating among hyainailourine taxa. For example, dP³s are known for at least three hyainailourines: *Leakitherium*, *Paroxyaena*, and *Pterodon dasyuroides*. Among these, *Leakitherium* exhibits the most individuated metacone on dP³ with a distinct furrow on the buccal surface of the tooth defining the bases of the paracone and metacone. In *Pterodon* and *Paroxyaena* the metacone is a low cusp with a distally pointing apex, lacking any deep furrow separating it from the paracone.

Leakitherium offers additional data on deciduous dental replacement order in Hyainailouroidea. The KNM-RU 15182 (Figure 3) specimen suggests that in *Leakitherium*, dP³ was retained longer than dP⁴. This deciduous replacement order is consistent with the deciduous replacement order that Bastl and Nagel (2013) observed in *Hyaenodon*, a hyaenodont taxon that likely diverged from the clade that includes Hyainailouroidea during the late Cretaceous or early Paleocene (Borths et al., 2016).

Subfamily TERATODONTINAE Savage, 1965
Genus ANASINOPA Savage, 1965

Type species. *Anasinopa leakeyi* Savage, 1965.

Other included species. *Anasinopa libyca* Morales, Brewer, and Pickford, 2010.

Anasinopa leakeyi Savage, 1965
Figures 4-5, Tables 1-2

Referred specimens. KNM-RU 2385, left maxilla fragment with dP², dP³, and dP⁴ (Rusinga Island, Kenya).

Description

The description of the maxillary dentition of *Anasinopa leakeyi* (KNM-RU 2385, Figure 4) is based on a cast deposited in the Rusinga collection at the National Museums of Kenya. A note on the specimen label speculates the original may

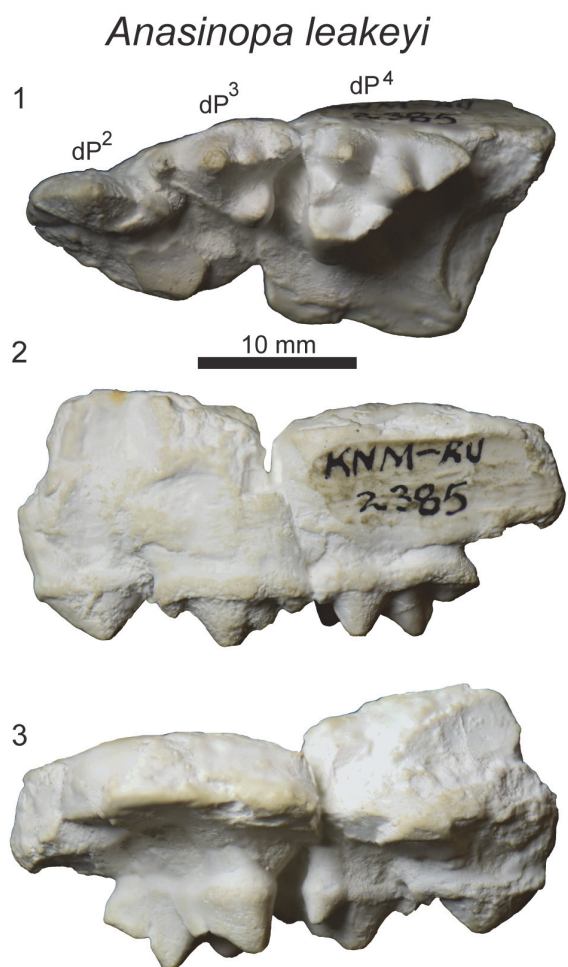


FIGURE 4. *Anasinopa leakeyi* left maxilla cast with dP², dP³ and dP⁴ (KNM-RU 2385) from Rusinga Island (early Miocene), Kenya in **1**) occlusal view; **2**) buccal view; and **3**) lingual view. Scale bar is 10 mm.

have been lent to Savage, but the exact location of the original specimen is unknown. The specimen preserves dP², dP³, and dP⁴. There is an indentation on the buccal surface of the cast superior to the mesial root of dP³ that suggests the infraorbital foramen is preserved in the original, though it is not as clear on the cast. The morphology of the dental crowns appears to be accurately captured, with no evidence of bubbles in the plaster, making the detailed description of the deciduous upper dentition possible based on the cast of KNM-RU 2385.

The dP² is a buccolingually compressed tooth with a long, low paracone with a height less than half the mesiodistal length of the tooth. A small metastyle is present at the distal point of the tooth, forming a distinct, but small notch between the paracone and metastyle. A clear buccal cingulum traces the buccal surface of the tooth from the

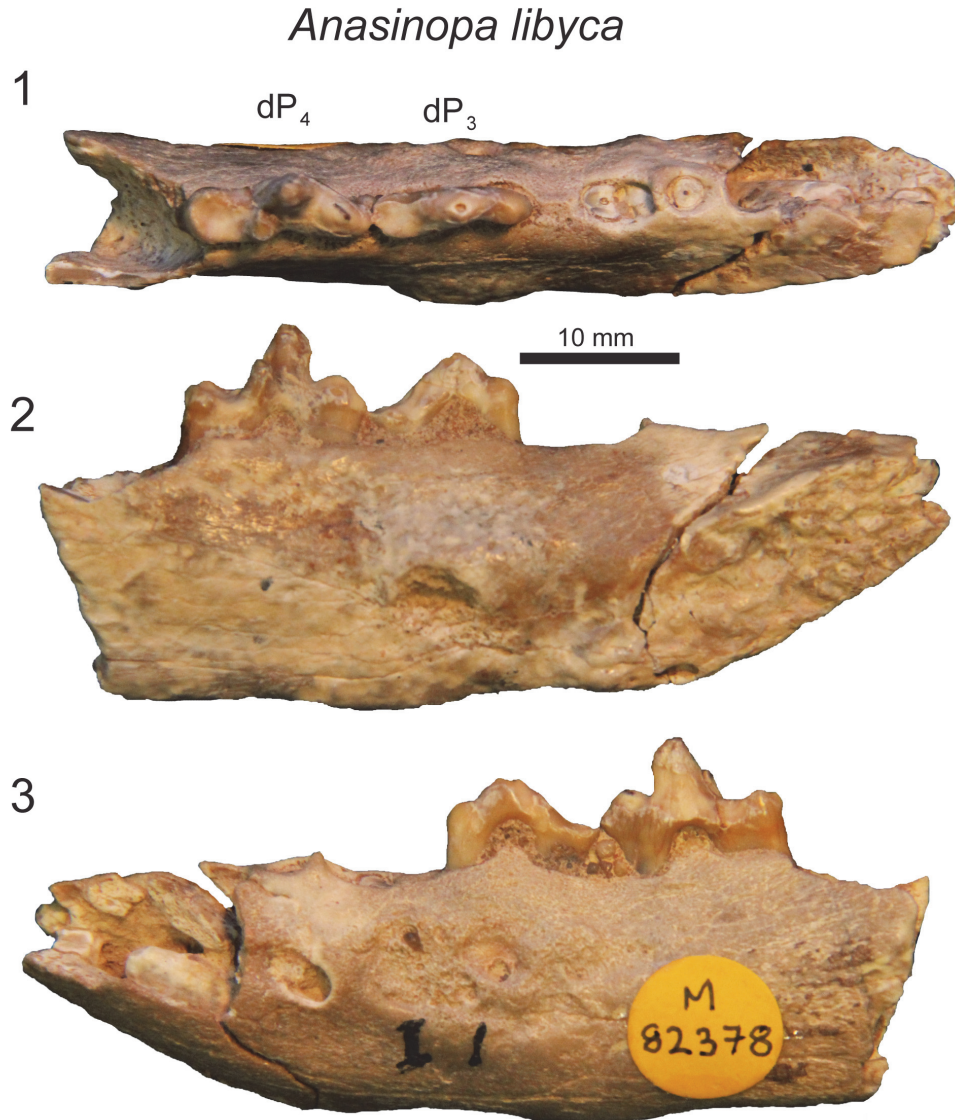


FIGURE 5. *Anasinopa libyca* left dentary with dP₃ and dP₄ from Gebel Zelten (middle Miocene), Libya (BMNH M82378) in **1**) occlusal view; **2**) lingual view; **3**) buccal view. Scale bar is 10 mm.

parastyle to the metastyle. The mesiodistal length of the dP² metastyle is less than 25% of the total length of the tooth. The buccal surface of the metastyle is braced by the parastyle of dP³ such that the buccal face of the dP² metastyle is blocked by the parastyle of dP³ in buccal view.

The dP³ bears a mesiodistally elongate parastyle that is the same length as the metastyle. The parastyle is a single, distinct cusp that forms a notch where it intersects the preparacrista. The preparacrista rises to the apex of the paracone at a 45 degree angle. The paracone is the tallest cusp

on dP³. The postparacrista is buccolingually compressed, as is the metacone which is a long, low cusp that forms a notch with the postparacrista. The metacone is less than half the height of the paracone. The metastyle forms a distinct carnassial notch with the metacone and rises to the same height as the parastyle and is only half the height of the metacone. On the distobuccal surface of dP³ is a shallow buccal basin framed by the metacone, metastyle, and buccal cingulum. The protocone projects distolingually from the base of the paracone. The protocone is the same height as the carnassial notch of dP³. In occlusal view the proto-

cone is triangular, with the mesial and distal margins of the cusp intersecting at a wide angle with no indication of a metaconule or paraconule. A thin lingual cingulum connects the parastyle to the protocone. The metastyle of dP³ contacts the mesial-most point of the parastyle of dP⁴.

The mesiodistal length of dP⁴ is only slightly longer than dP³. The parastyle of dP⁴ is smaller and more cingulum-like than the distinct, cusp-like parastyle on dP³. On dP⁴ a distinct buccal cingulum connects the parastyle to the metastyle. Distal to the parastyle, the paracone and metacone are divergent cusps from their bases to their apices. The paracone is only slightly buccolingually compressed, and its base is circular in cross section. The metacone is more buccolingually compressed than the paracone and is more lingually positioned than the paracone. The postmetacrasta is sectorial, forming a deep carnassial notch with the metastyle. The mesiodistal length of the metastyle is subequal to the mesiodistal length of the metacone base. The metastyle is blade-like with a distinct convex crista that gently inflects distally. The metastyle does not connect to the protocone. Instead, a large metaconule that is the same height as the carnassial notch arises near the distal base of the metacone. A small, but distinct notch is formed between the metaconule and protocone. The protocone is a tall cusp that is subequal in height to the paracone. The apex of the protocone points in a mesiobuccal direction. Compared with the protocone of dP³, the protocone of dP⁴ is mesially shifted and buccolingually aligned with the paracone in occlusal view. The mesial margin of the protocone forms a small notch with the paraconule. The paraconule is as large and well-defined as the metaconule. A thin lingual cingulum connects the paraconule to the parastyle. The large protocone, paraconule, metaconule, and divergent paracone and metacone frame a wide and deep trigon basin. The mesial roots of M¹ are preserved on the specimen, indicating the protocone of M¹ projected more lingually than the protocone of dP⁴. The mesiobuccal root of M¹ also indicates the metastyle of dP⁴ was aligned with the parastyle of M¹.

Morales et al. (2010) described portions of the lower deciduous dentition of *Anasinopa libyca* from the early middle Miocene of Libya. Here we provide additional description of this specimen (Figure 5), discovered by R. J. G. Savage, which preserves the morphology dP₃ and dP₄. There is a short diastema between the distal alveolus of dP₂ and dP₃.

dP₃ is buccolingually compressed with a mesiodistally extensive paraconid. dP₃ is heavily abraded, but there was a distinct talonid basin. Like dP₃, the trigonid of dP₄ is buccolingually compressed. The bases of the paraconid and protoconid are subequal in length. The postprotocristid slopes to a small metaconid at the distal-most margin of the protoconid base. The small metaconid is less than half the height of the protoconid. The talonid basin of dP₄ is shallow, and enclosed lingually by the entocristid, which connects with the base of the metaconid. The talonid basin of dP₄ is demarcated by a low, but distinct hypoconid and hypoconulid and a slight entoconid that grades into the entocristid.

Remarks

Recent phylogenetic analyses resolve *Anasinopa* within Teratodontinae, an entirely Afro-Arabian clade (Solé et al., 2014; Rana et al., 2015; Borths and Seiffert, 2017). In the topologies described by Borths et al. (2016) and Borths and Seiffert (2017) Teratodontinae is the sister clade of Hyainailouridae (Apterodontinae + Hyainailourinae). Teratodontinae is generally characterized by dental features shared with mesocarnivores including divergent paracones and metacones, basined talonids, and the presence of metaconids. However, within Teratodontinae, some taxa, like *Anasinopa*, combine this mesocarnivorous morphology with hallmarks of hypercarnivores like exaggerated metastyles and tall, buccolingually compressed metacones. Borths et al. (2016) demonstrated that teratodontines specifically converged with the hypercarnivorous dental morphology of Hyaenodontinae. Despite convergent features associated with hypercarnivory, synapomorphies between the deciduous dentition of *Anasinopa* and the deciduous dentition of other teratodontines consistently place this hypercarnivorous, wolf-sized hyaenodont within Teratodontinae.

In several recent phylogenetic analyses (Rana et al., 2015; Borths and Seiffert, 2017) *Dissopsalis* and *Anasinopa* are closely related taxa within Teratodontinae and both taxa are found in early to middle Miocene sites. The two genera differ in size, with *Anasinopa* slightly smaller than *Dissopsalis*. The adult dentitions of *Dissopsalis* and *Anasinopa* both mix mesocarnivorous and hypercarnivorous dental features, with M₁ and M₂ retaining the well-developed talonid basins of mesocarnivores, but the talonid of M₃ reduced to a single cusp and the carnassial blade of M₃

expanded as would be expected in hypercarnivores. When *Dissopsalis* and *Anasinopa* are directly compared, *Dissopsalis* has more exaggerated hypercarnivorous dental features, with more reduced paracones on the upper molars and more elongate carnassial blades.

The maxillary specimen, KNM-RU 2385 (Figure 4), is consistent in size with *Anasinopa* and the expanded trigon basins, mesiodistally shorter metastyles, and widely divergent paracone and metacone on dP⁴ are also consistent with the adult dental morphology of *Anasinopa*. The deciduous dentition of *Anasinopa* and *Dissopsalis* are similar, although several characters can be used to distinguish these taxa. *Anasinopa* has a dP³ metacone that is mesiodistally shorter than the dP³ metacone of *Dissopsalis*. Further, the metastyle on dP³ in *Anasinopa* is also mesiodistally shorter than the dP³ metastyle of *Dissopsalis*. The dP³ buccal cingulum of *Anasinopa* is wider and more distinct than is the buccal cingulum of *Dissopsalis*. Like the metastyle on dP³, the metastyle of dP⁴ in *Anasinopa* is relatively shorter than the metastyle on dP⁴ in *Dissopsalis*. The protocone on dP⁴ of *Anasinopa* bears a more distinct paraconule and metaconule than the protocone of dP⁴ in *Dissopsalis*, and the margins of the protocone in *Anasinopa* meet at a wider angle, giving the protocone a broader, triangular shape in occlusal view than the mesiodistally narrowed dP⁴ protocone of *Dissopsalis*.

Masrasector is also nested within Teratodontinae and is closely related to *Anasinopa*. *Anasinopa* is larger than *Masrasector*, but the two taxa share divergent metacones and paracones on dP⁴. Also on dP⁴ in both *Masrasector* and *Anasinopa*, the metacone is lingually placed relative to the paracone rather than mesiodistally aligned with the paracone as it is in *Dissopsalis*, *Leakitherium*, and *Apterodon*. The divergent dP⁴ paracones, metacones, and protocones of both *Masrasector* and *Anasinopa* surround broad trigon basins.

In teratodontines the M¹ and M² paracones are subequal to or lower than the metacones, leaving the metacone as the lead piercing cusp on the molars. In *Anasinopa*, dP⁴ anticipates the morphology of the adult molars by exhibiting a slightly taller metacone than paracone, morphology that is shared with the dP⁴ of *Masrasector*. The dP⁴ of *Anasinopa* shares with the dP⁴ of the teratodontines *Brychotherium*, *Masrasector*, and *Metasinopa*, a broad shelf between the metastyle, metacone, and buccal cingulum. *Dissopsalis* lacks this broad distal buccal shelf.

The dentary of *Anasinopa libyca* preserves dP₃ and dP₄ (Figure 5). Morales et al. (2010) noted *A. libyca* is 10 to 25% smaller than *A. leakeyi*, the species to which we refer KNM-FT 3357. dP₄ in *A. libyca* shares with the dP₄ of *Masrasector* and *Metasinopa* a distinct metaconid that is only slightly lower than the paraconid. These three teratodontines also share a mesiodistally elongate talonid basin with distinct hypoconids and hypoconulids. *A. libyca* and *Metasinopa* differ from *Masrasector* in lacking distinct entoconids on the lingual margin of the talonid basin. Instead, *A. libyca* and *Metasinopa* both exhibit smooth entocristids that close the lingual margin of the talonid.

Genus DISSOPSALIS Pilgrim, 1910

Type species. *Dissopsalis carnifex* Savage, 1965.

Other included species. *Dissopsalis pyroclasticus* Barry, 1988.

Dissopsalis pyroclasticus Barry, 1988

Figure 6, Table 1

Referred specimens. KNM-FT 3357, left maxilla fragment with dP³ and dP⁴ (Fort Ternan, Kenya).

Description

The maxillary specimen, KNM-FT 3357 (Figure 6), is referred to *Dissopsalis* based on comparisons with other material referred to *Dissopsalis* from Fort Ternan, including KNM-FT 3562, a close size match to KNM-FT 3357. It is possible this represents the upper deciduous dentition of *Anasinopa*, but based on morphological comparisons detailed below we identify the Fort Ternan specimen as a maxillary fragment of *Dissopsalis*, and refer the slightly smaller KNM-RU 2385 (Figure 4) to *Anasinopa*.

Only fragmentary portions of the lateral margin of the maxilla are preserved on KNM-FT 3357, including the inferior margin of the infraorbital foramen superior to the mesial root of dP³. A single alveolus of P¹ is preserved at the rostral-most portion of the specimen. Based on the fragmentary preservation of this alveolus, it is difficult to determine whether this tooth had a single root in the single alveolus, or if this is the distal of two roots. Both alveoli of dP² are preserved. The distal alveolus of that tooth position exhibits a larger circumference than does the mesial root, crowding the mesial margin of dP³. The morphology of this distal alveolus indicates dP² and dP³ would have been closely packed with the metastyle of dP² braced buccally by the parastyle of dP³.

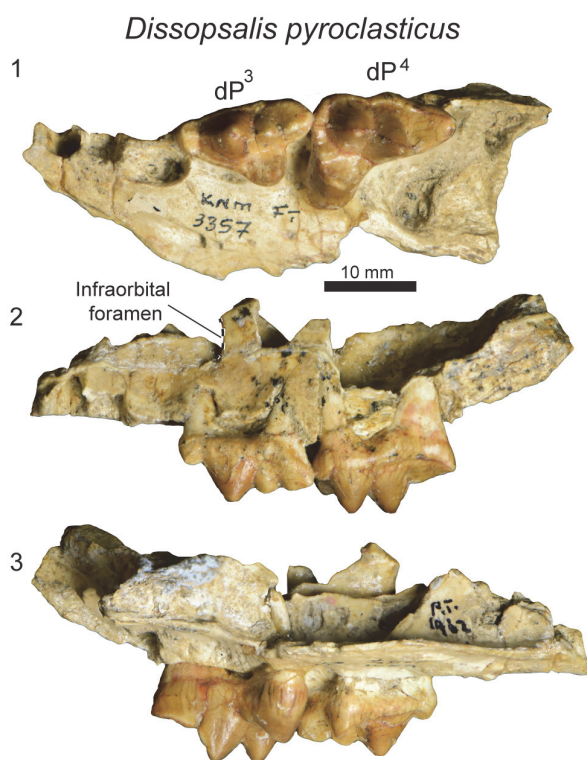


FIGURE 6. *Dissopsalis pyroclasticus* left maxilla with dP³ and dP⁴ (KNM-FT 3357) from Fort Ternan (early Miocene), Kenya in **1)** occlusal view; **2)** buccal view; and **3)** lingual view. Scale bar is 10 mm.

The entire crown of dP³ is preserved. The mesiodistal length of the parastyle and metastyle are subequal. The parastyle and metastyle are mesiodistally aligned and are intersected at a perpendicular angle by the protocone. The parastyle, metastyle and protocone are distinct cusps, but each is relatively low compared to the paracone, which is the tallest cusp on the tooth. The mesiodistal length of the paracone is subequal to the height of the paracone, making the cusp appear long and low in buccal view. The preparacrista is twice the length of the postparacrista, which intersects the metacone. The metacone is distinct, only half the height of the paracone, and exhibits greater convexity along the buccal surface than the lingual surface. The metacone forms a shallow carnassial notch with the short, low metastyle. The parastyle and metastyle are connected to the large protocone, defining the mesial and distal margins of the wide trigon basin. The protocone on dP³ is distally oriented, defining a relatively narrow space between the lingual aspects of dP³ and dP⁴.

In *Dissopsalis* (KNM-FT 3357, Figure 6) dP⁴ is mesiodistally only slightly longer than dP³,

though the relative proportions of the cusps are very different with the distinct parastyle mesiodistally shorter than the metastyle and the protocone shifted mesially so that it is lingual to the paracone. The small, cusp-like parastyle connects the distinct buccal cingulum of dP⁴ to the paraconule. The paracone and metacone are fused for about half of their height, then the apices diverge, with both oriented perpendicular to the palate. The paracone and metacone are subequal in mesiodistal length, and the metacone is slightly taller than the paracone. Both the metacone and paracone are buccolingually compressed. The distal margin of the metacone is the most compressed and sectorial portion of these cusps. The metacone forms a distinct, though shallow, carnassial notch where it intersects the metastyle. The metastyle is lower than the metacone and comparable in height to the parastyle. The protocone is a mesiodistally broad cusp that is subequal in height to the parastyle. The protocone frames the lingual margin of a deep trigon basin that is buccally defined by the paracone, mesially defined by a distinct paraconule, and distally defined by a distinct metaconule.

Remarks

Dissopsalis is one of the last teratodontines documented in the fossil record (Solé et al., 2015) and is also one of the most hypercarnivorous, as reflected by the elongate metastyle and buccolingually compressed metacone on dP⁴ in KNM-FT 3357 (Figure 6). The dP³ of *Dissopsalis* shares with *Masrasector*, *Metasinopa*, *Anasinopa*, and *Pakakali* a low metacone and a mesiodistally elongate metastyle. The dP³ of *Dissopsalis* and *Anasinopa* are distinct from *Masrasector* and from the other hyainailouroid dP³ specimens considered in this study by having a mesiodistally elongate paracone with a low buccal profile and a mesiodistally elongate metacone. The carnassial notch of dP³ in *Dissopsalis* also differs from all other hyainailouroids by being relatively shallow rather than defined by a deep notch that almost divides the metastyle and metacone down to the buccal cingulum.

In teratodontines the M¹ and M² paracones are subequal to or lower than the metacones, leaving the metacone as the lead piercing cusp on the molars. In *Dissopsalis* the dP⁴ anticipates the morphology of the adult molars in exhibiting a slightly taller metacone than paracone, morphology that is shared with the dP⁴ of *Masrasector* and *Anasinopa*. Unlike *Anasinopa*, the bases of the paracone

and metacone on dP⁴ in *Dissopsalis* are partially fused, also anticipating the more fused paracone and metacone found on the molars of *Dissopsalis*. The dP⁴ of *Dissopsalis* differs from the dP⁴ of the teratodontines *Brychotherium*, *Masrasector*, and *Metasinopa*, in having a constricted space between the metastyle, metacone, and buccal cingulum. Overall, the more exaggerated hypercarnivorous characters evident on the deciduous dentition of *Dissopsalis* reveal dietary adaptations that are important for interpreting the biology of one of the latest surviving hyaenodonts in Afro-Arabia.

Genus MASRASECTOR Simons and Gingerich, 1974

Type species. *Masrasector aegypticum* Simons and Gingerich, 1974.

Other included species. *Masrasector ligabuei* Crochet, Thomas, Roger, and Al-Sulaimani, 1990; *Masrasector nananubis* Borths and Seiffert, 2017.

Masrasector nananubis Borths and Seiffert, 2017
Figures 7-9, Tables 1-2

Referred specimens. DPC 20882, right maxilla fragment with dP³ and dP⁴ (Fayum Depression, Jebel Qatrani Formation, Quarry L-41); DPC 13837, right maxilla fragment with dP³, dP⁴, M¹ (Fayum Depression, Jebel Qatrani Formation, Quarry L-41); DPC 18276, right dentary with dP₂, dP₃, dP₄ (Fayum Depression, Jebel Qatrani Formation, Quarry L-41). Note: These specimens were all found in isolation in Quarry L-41 and are not likely associated.

Description

The upper deciduous dentition of *Masrasector nananubis* is best represented by the two maxillary fragments we identify here: DPC 20882 and DPC 13837 (Figure 7). Both are right maxillary fragments preserving portions of dP³ and dP⁴. DPC 13837 further preserves M¹, illustrated here to highlight some of the differences between dP⁴ and M¹.

The infraorbital foramen is preserved in both specimens superior to the mesial root of dP³. The parastyle of dP³ is elongate and buccolingually compressed into a narrow crista that connects with the preparacrista of the paracone. The dP³ is best preserved on DPC 20882 where the parastyle is mesiodistally subequal in length to the metastyle and is subequal in height to the apex of the metastyle. A thin buccal cingulum connects the parastyle to the metastyle. The paracone is the tallest cusp on dP³. The apex of the paracone forms an

equilateral triangle in buccal view. The metacone is half the height of the paracone and it is closely appressed to the paracone, though it is a distinct cusp with a shallow furrow defining the margins of the metacone where it fuses with the paracone. In occlusal view, the metacone is positioned slightly lingual to the apex of the paracone. The metacone forms a deep carnassial notch at the juncture with the sectorial metastyle. A thin shelf is formed between the metastyle, the metacone, and the buccal cingulum. The protocone is mesiodistally narrow and isolated from the parastyle and metastyle.

The crown of dP⁴ is best preserved on DPC 20882 (Figure 7). The parastyle is a distinct cusp that is mesiodistally shorter than the metastyle. As on dP³ and M¹ (DPC 13837) the parastyle and metastyle of dP⁴ are connected by a distinct buccal cingulum. The paracone and metacone are fused at their bases and diverge near the midpoint of their height. The paracone and metacone are subequal in height, are slightly buccolingually compressed and have similar basal diameters. The paracone is proximate to the buccal cingulum with the metacone positioned more lingually. The post-metacrista meets the metastyle at a deep carnassial notch. A wide basin is formed between the sectorial metastyle, the buccal cingulum, and the bases of the paracone and metacone. The buccal cingulum traces a shallow ectoflexus. The protocone is mesially oriented and lingually aligned with the mesial margin of the parastyle. A thin mesial cingulum connects the parastyle to the protocone, but the protocone is not connected to the metastyle. The protocone is a mesiodistally broad cusp that projects beyond the divergence of the paracone and metacone.

Maxillary specimens of *Masrasector* (Figure 7) were μ -CT scanned, revealing that the developing permanent dentition has not reached the bell stage of differentiation in DPC 20882, a specimen that only preserves dP³ and dP⁴. DPC 13837 (Figure 7) preserves a fully erupted M¹ with open roots, and developing portions of P³ and P⁴ that both advanced into the bell phase of tooth differentiation. The paracone of P³ has coalesced in the crypt, framed by the roots of dP³. The paracone of P⁴ had only just started to coalesce in the crypt, evidence that in *Masrasector*, P³ likely erupted before P⁴.

The lower deciduous dentition of *Masrasector nananubis* was described by Borths and Seiffert (2017), though that previous study did not detail

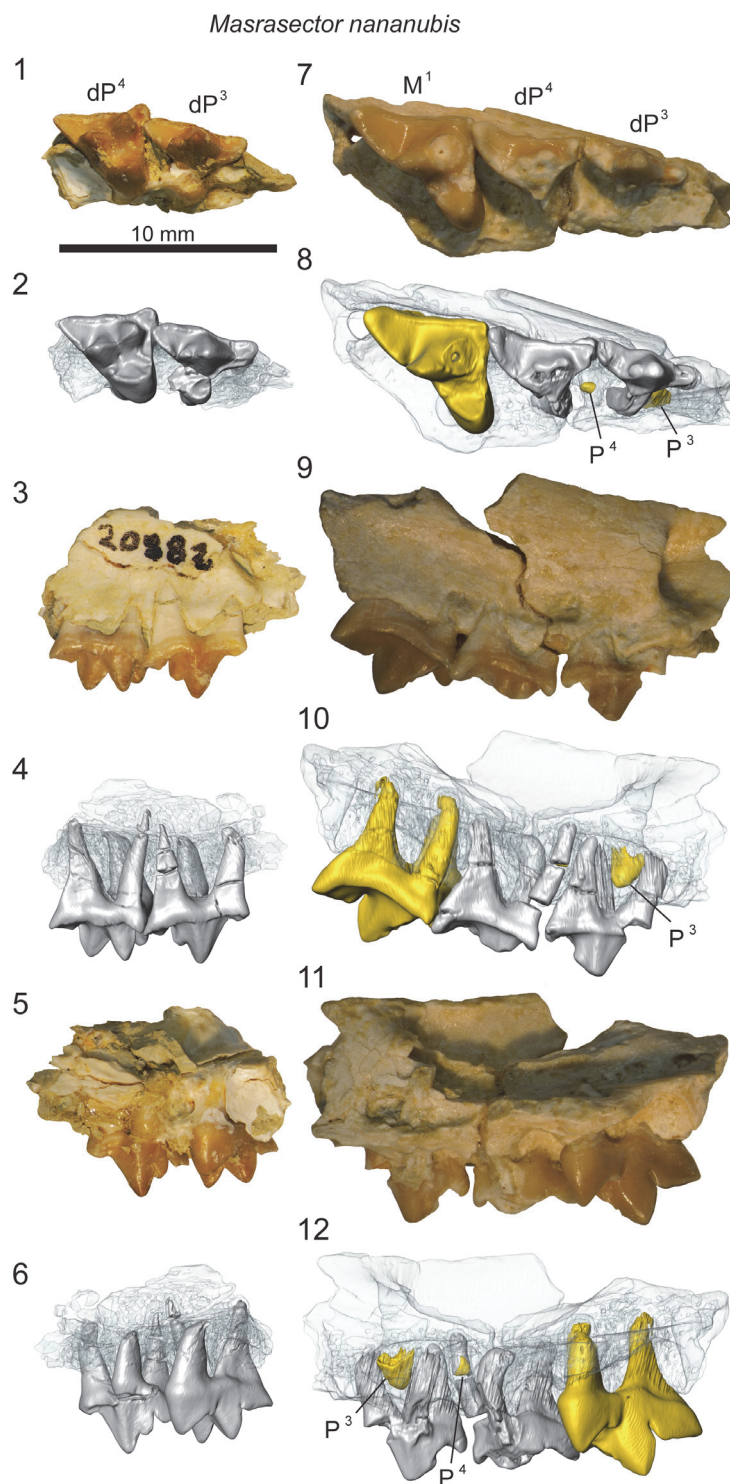


FIGURE 7. *Masrasetor nananubis* left maxillae from Locality 41 (latest Eocene), Fayum Depression, Egypt. Original specimens figured with digital models based on μ -CT scans reconstructed in Avizo. Maxilla rendered transparent to reveal developing dentition. Grey, deciduous dentition. Yellow, permanent dentition. DPC 20882 is a left maxilla fragment that preserves dP³ and dP⁴ and no indication of developing permanent dentition. **1)** specimen occlusal view; **2)** model occlusal view; **3)** specimen buccal view; **4)** model buccal view; **5)** specimen lingual view; **6)** model lingual view. DPC 13837 is a left maxilla fragment that preserves erupted dP³, dP⁴, and M¹ and P³ and P⁴ developing in crypts. **7)** specimen occlusal view; **8)** model occlusal view; **9)** specimen buccal view; **10)** model buccal view; **11)** specimen lingual view; **12)** model lingual view. Scale bar is 10 mm.

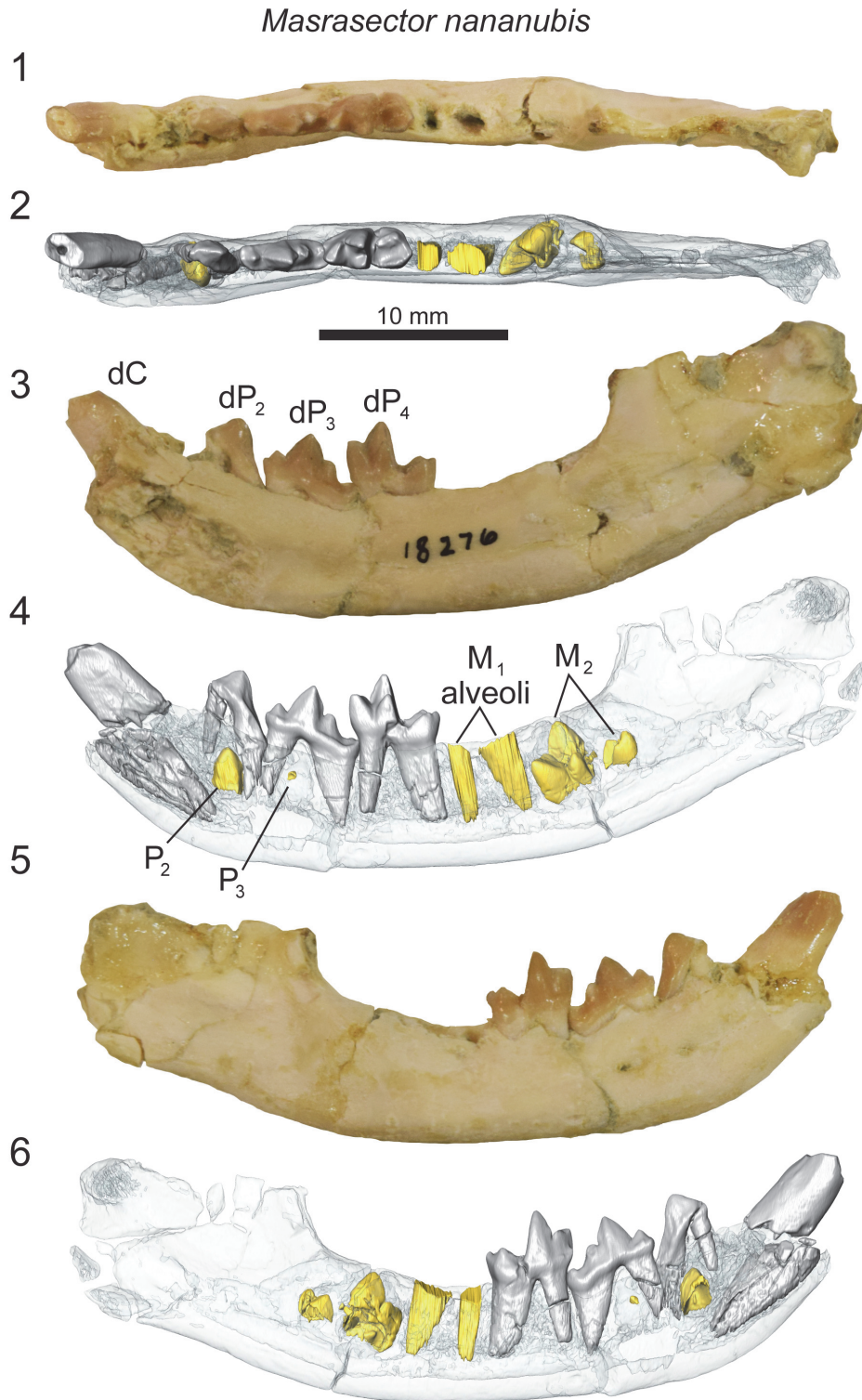


FIGURE 8. *Masrasector nananubis* right dentary with erupted dC, dP₂, dP₃, and dP₄, M₁ alveoli and P₂, P₃, and M₂ in crypts (DPC 18276) from Locality 41 (latest Eocene), Fayum Depression, Egypt. Original specimen figured with digital model based on μ -CT scans reconstructed in Avizo. Dentary rendered transparent to reveal developing dentition. Grey, deciduous dentition. Yellow, permanent dentition. **1)** specimen occlusal view; **2)** model occlusal view; **3)** specimen lingual view; **4)** model lingual view; **5)** specimen buccal view; **6)** model buccal view. Scale bar is 10 mm.

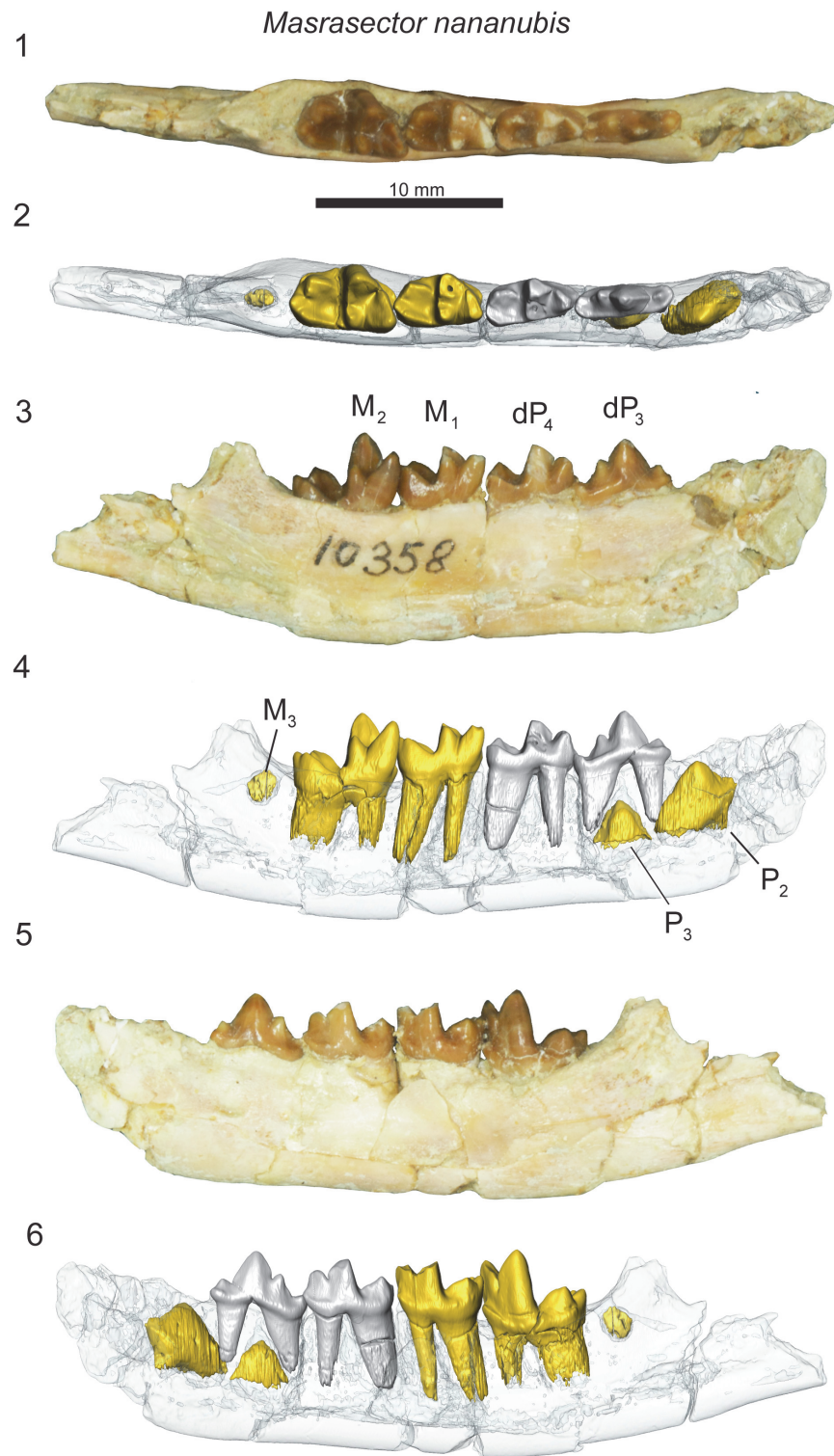


FIGURE 9. *Masrasector nananubis* left dentary with erupted dP_3 , dP_4 , M_1 and M_2 and P_2 , P_3 , and M_3 in crypts (DPC 10358) from Locality 41 (latest Eocene), Fayum Depression, Egypt. Original specimen figured with digital model based on μ -CT scans reconstructed in Avizo. Dentary rendered transparent to reveal developing dentition. Grey, deciduous dentition. Yellow, permanent dentition. **1)** specimen occlusal view; **2)** model occlusal view; **3)** specimen lingual view; **4)** model lingual view; **5)** specimen buccal view; **6)** model buccal view. Scale bar is 10 mm.

the development of the permanent dentition revealed by μ -CT. The dentary specimen DPC 18276 (Figure 8) preserves the crowns of the deciduous canine, dP₂, dP₃, dP₄, and the alveoli of M₁. The developing buds of P₂, P₃, and M₂ are preserved in their crypts. Of these coalescing permanent teeth, M₂ is most advanced, with the enamel bells of the trigonid and talonid fully formed; it likely would have erupted before the other developing dentition. The P₂ is framed by the roots of dP₂. The crown of P₂ is oriented oblique to the body of the dentary. A tiny portion of the differentiated enamel of the P₃ paraconid is visible between the roots of dP₃. The dentary specimen DPC 10358 (Figure 9) is from a developmentally older individual than DPC 18276 (Figure 8). DPC 10358 preserves a fully erupted M₂, though the roots are not fully differentiated, the crown of P₂ is nearly completely developed and it is oriented subparallel to the mandibular corpus, and P₃ is advanced into the enamel bell phase. Distal to M₂, a dense mass is visible in the μ -CT scans, interpreted as the early differentiation of M₃. Neither *Masrasector* dentary specimen preserves any portion of the differentiated tooth bud of P₄. Taken together, these specimens suggest the following order of permanent dental eruption in *Masrasector nananubis*: M₁, M₂, P₂, P₃, M₃, and P₄.

Remarks

Masrasector nananubis is much smaller than the other hyainailouroids discussed in this study. Whereas the metacone is immediately distal to the dP₃ paracone in *Anasinopa*, *Dissopsalis*, and *Leakitherium*, the dP₃ metacone in *Masrasector nananubis* is slightly lingually offset, a feature shared with *Metasinopa*. The metacone is lingually offset from the paracone even more dramatically on the dP₄ of *M. nananubis*, a feature also shared with the teratodontines *Brychotherium*, *Anasinopa*, and *Metasinopa*, but not *Dissopsalis*. The lingually projecting protocone of the dP₄ in *M. nananubis* frames a broad trigon basin, a feature also shared with *Brychotherium*, *Anasinopa*, and *Metasinopa*, but not with *Dissopsalis* (which exhibits a dP₄ protocone that projects mesially and is not framed by the bases of both the metacone and paracone). This trigon basin diversity within Teratodontinae may reflect dietary differences within the clade, with *Masrasector* acting as a mesocarnivore and *Dissopsalis* acting as a hypercarnivore, though *Dissopsalis* retains some mesocarnivorous dental

traits that help distinguish the taxon from the hyainailouroids.

Genus METASINOPA Osborn, 1909

Type species. *Metasinopa fraasi* Osborn, 1909

Other included species. *Metasinopa ethiopia* Andrews, 1906; *Metasinopa napaki* Savage, 1965.

Metasinopa sp.

Figures 10-11, Tables 1-2

Referred specimens. DPC 10199, associated cranial fragments with dP₃, dP₄, M₁ (Fayum Depression, Jebel Qatrani Formation, Quarry V); DPC 4544, P₂, dP₄, M₁-M₃ (Fayum Depression, Jebel Qatrani Formation, Quarry V). Note: The specimens were found in the same quarry, but are not likely associated with the same individual.

Description

The enamel on both dP₃ and dP₄ is smooth and thin (DPC 10199; Figure 10). The parastyle of dP₃ is elongate and buccolingually compressed. The paracone of dP₃ is the largest cusp on the tooth, with a paracone basal diameter twice the size of the basal diameter of the buccolingually

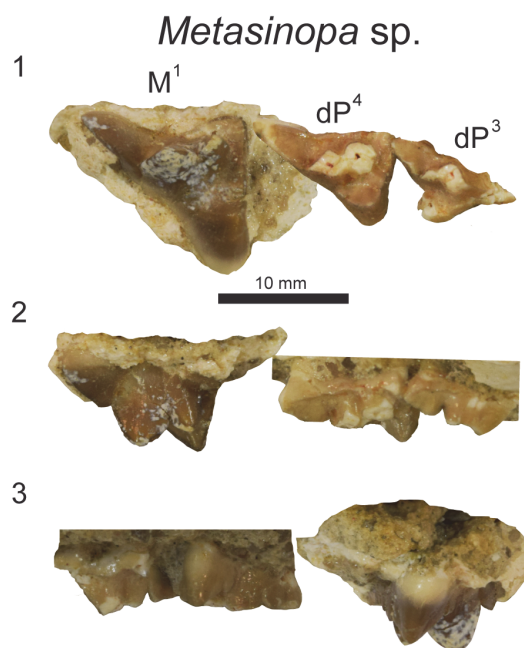


FIGURE 10. *Metasinopa* sp. left maxilla fragments with dP₃, dP₄, and M₁ (DPC 10199) from Quarry V (early Oligocene), Fayum Depression, Egypt in **1**) occlusal view; **2**) buccal view; and **3**) lingual view. Note that there is matrix around the roots of the specimens that has been cropped to make the dentition easier to view. Scale bar is 10 mm.

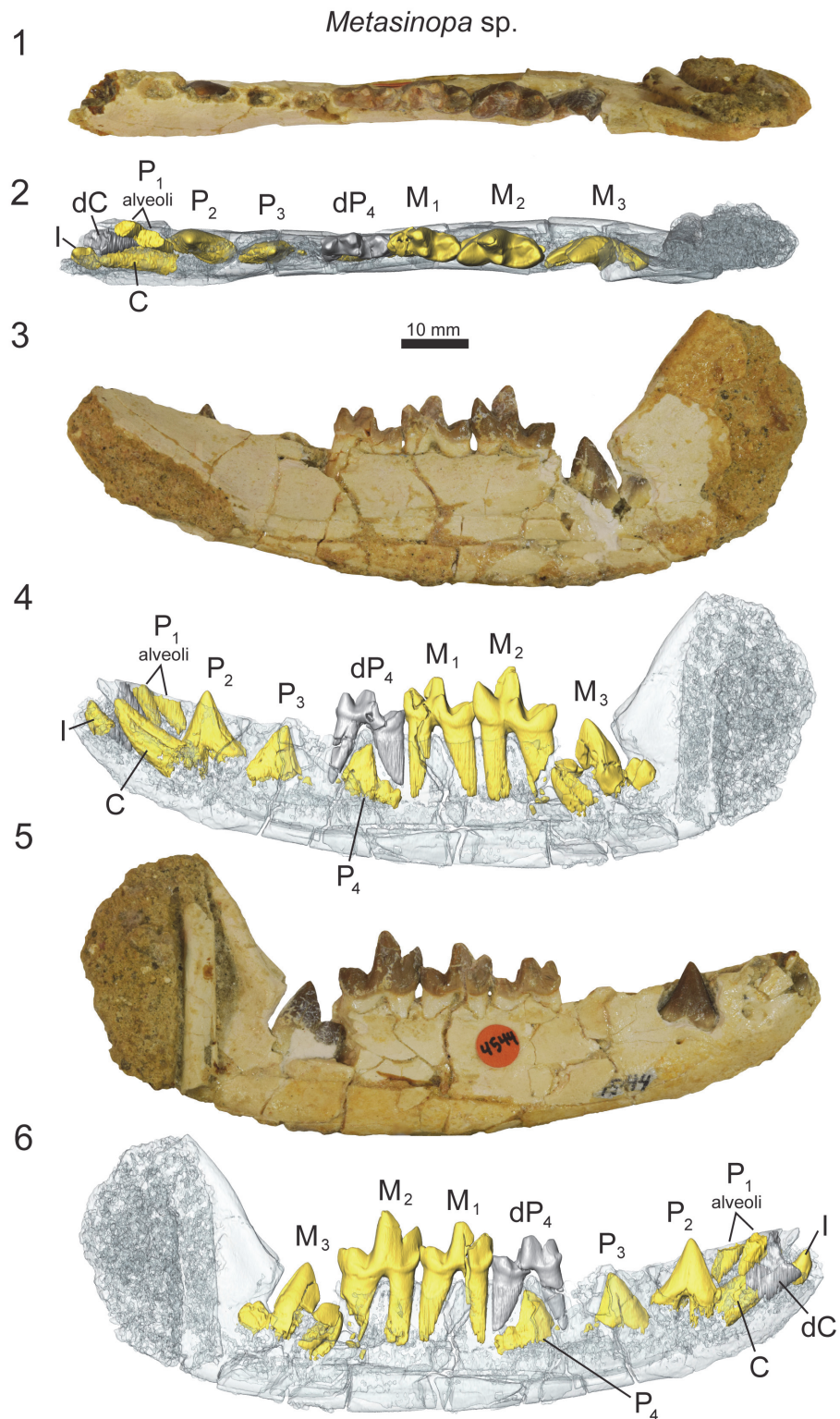


FIGURE 11. *Metasinopa* sp. right dentary with dC, dP₄, M₁, M₂ and I, C, P₂, P₃, P₄ M₃ in crypts (DPC 4544) from Quarry V (early Oligocene), Fayum Depression, Egypt. Original specimen figured with digital model based on μ -CT scans reconstructed in Avizo. Dentary rendered transparent to reveal developing dentition. Yellow, permanent dentition. **1)** specimen occlusal view; **2)** model occlusal view; **3)** specimen lingual view; **4)** model lingual view; **5)** specimen buccal view; and **6)** model buccal view. Scale bar is 10 mm.

compressed metacone. The apex of the metacone is lightly worn and did not much exceed the maximum height of the metastyle. A very deep carnassial notch separates the metastyle from the metacone. The mesiodistal width of the protocone is subequal in diameter to the paracone. The protocone is isolated from the metastyle, but connected to the parastyle by a thin cingulum.

The dP⁴ exhibits a reduced parastyle compared to the dP³ and an elongate metastyle. The mesiodistal length of the dP⁴ metastyle is subequal to the mesiodistal diameter of the paracone and metacone base. Along the buccal margin of the metastyle is a shallow ectoflexus traced by a slight buccal cingulum. The apices of the paracone and metacone are not preserved, but the bases of these cusps indicate the paracone was conical and the metacone was more buccolingually compressed with a blade-like postmetacrista. The protocone of dP⁴ projects mesially and is nearly aligned with the mesial edge of the parastyle. The trigon basin is mesiodistally broad and framed by a distinct paraconule, metaconule and protocone.

In contrast to dP⁴, the mesiodistal length of the metacone of M¹ is significantly longer than the base of the paracone, and the paracone is reduced to a mesially directed cusp that is lower than the metacone. The ectoflexus of M¹ is deeper than the ectoflexus of dP⁴, and the buccal cingulum is thin to absent.

A dentary referable to *Metasinopa* (DPC 4544; Figure 11) was also discovered at Quarry V. The buccal portions of the dentary were prepared away, exposing the buccal faces P₂ and M₃. On the buccal aspect of the dentary, mental foramina are present inferior to the alveoli of both P₁ and P₂. The alveoli of P₁ indicate that the tooth had two roots and was aligned with the base of canine. The alveoli of dP₃ are also preserved. The dP₄ is buccolingually narrow compared with M₁, and the paraconid of dP₄ is aligned with the protocone. This contrasts with the more lingually oriented paracone of M₁. A low metaconid is retained on dp₄, a cusp also present, and at nearly the same absolute size, on each of the molars. The talonid of dP₄ is closed lingually by a complete entocristid that connects to the base of the metaconid. The hypoconid is large and well developed, and the hypoconulid is a distinct distal cusp on the talonid. There is substantial wear on the protoconid and paraconid of dP₄.

The μ -CT scans reveal that all of the permanent dentition were present in DPC 4544 (Figure 11). A permanent incisor with three distinct tines is present mesial to the deciduous canine. The specimen does not preserve the complete incisor row, making it difficult to determine the precise incisor locus represented in this specimen. The incisor root is open, though the crown is complete. The permanent canine is developing in the crypt, lingual to the root of the deciduous canine. The crown of P₂, both paraconid and talonid, and portions of the roots are fully developed and the apex of the tooth is preserved superior to the alveolar margin. The enamel crown of P₃ is almost entirely differentiated in the crypt and the mesial root is partially coalesced, though portions of the talonid have not fully developed. The apex of P₃ protrudes nearly to the alveolar margin. The crown and talonid of P₄ are almost fully developed, though no portions of the roots have differentiated and the roots of dP₄ are complete. Both M₁ and M₂ are erupted and M₃ is in the crypt with the trigonid and talonid fully developed, though the roots are undifferentiated. The crypt is recessed in the dentary and there is not enough space in the tooth row to fully accommodate the crown of M₃, evidence that the body of the dentary had yet to elongate to accommodate the final lower molar. Given the development of each permanent tooth, the inferred eruption sequence for *Metasinopa* was likely: M₁, M₂, P₂, P₃, M₃, and P₄, then the canine with the mesial incisor erupting around the time of P₂.

Remarks

Metasinopa has been assigned several species that range from the late Eocene through the Miocene of Afro-Arabia. The diagnoses of these species are in need of close examination (Lewis and Morlo, 2010), but we refer specimens from the early Oligocene of the Jebel Qatrani formation to *Metasinopa* based on comparisons with the lower dentition preserved in *Metasinopa fraasi* (Osborn, 1909). Slightly larger than *Masrasector*, *Metasinopa* exhibits more hypercarnivorous dental features than does *Masrasector*, including a reduced dP₄ metaconid, more mesiodistally extensive metastyles on dP³ and dP⁴, and a taller, more buccolingually compressed metacone on M¹. *Metasinopa* shares with *Masrasector* a slightly lingually placed metacone on dP³ and dP⁴ that divides the protocone from the metastyle, and a tall dP⁴ protocone that projects beyond the point of divergence

between the metacone and paracone. *Metasinopa* shares with *Brychotherium* a deep ectoflexus on dP³ and dP⁴, not present in *Masrasector* or in the hyainailourids.

The dP₄ of *Metasinopa* is relatively more buccolingually compressed than the dP₄ of *Masrasector* with a narrower talonid relative to the trigonid. The dP₄ metaconid of *Metasinopa* is relatively smaller than that of *Masrasector*, with former rising only slightly above the alveolar margin.

PHYLOGENETIC ANALYSIS USING DECIDUOUS MORPHOLOGY

Phylogenetic Methods

A phylogenetic analysis was conducted to incorporate the deciduous dental morphology described in this study into a larger analysis of hyaenodont relationships. Deciduous dental morphology is heritable in mammals (Hughes et al., 2000; Townsend et al., 2012) and is a rich source of phenotypic character information. The character-taxon matrix is an expansion of hyaenodonts sampled by Borths et al. (2016), and Borths and Stevens (2017), building upon previous work by Polly (1996), Zack (2011), and Solé et al. (2014), adding additional characters of the deciduous dentition (14 deciduous, 148 total), and expanding the OTUs (84 total). Some of the characters incorporated into this analysis are modified from Bastl et al. (2014). The full character-taxon matrix used in this study is included as Appendix 1, with character descriptions and their references detailed in Appendix 2. Seventeen characters were ordered and are identified in Appendix 2.

This study incorporates deciduous dental material directly examined by the investigators. There is likely deciduous dental material that has been referred to one or more OTUs that were not scored for this particular analysis, particularly for OTUs from European localities. We included the taxa we were able to examine, and we invite later investigators to build upon this dataset with additional material referable to these taxa. Appendix 3 lists the specimens observed for each OTU as part of this study.

A model-based, Bayesian approach was used to analyze the character-taxon matrix in MrBayes (Ronquist et al., 2012) (Appendix 4). The goal of a Bayesian phylogenetic analysis is to recover a branch-length-scaled topology that maximizes the likelihood of observing the morphological character-taxon matrix. A Markov Chain Monte Carlo (MCMC) search explores different topologies with

varying branch lengths, searching for optimal topologies given the dataset. Topologies are held or rejected depending on their probability in proportion to their likelihoods. All topologies that have been accepted compose the posterior distribution of trees, except for the first 25%, which are rejected here as part of the burn-in period of the MCMC search. Posterior probabilities are proportional to the percentage of time the clade occurs in this posterior distribution. This method of phylogenetic inference has become commonplace in paleontological phylogenetic studies (e.g., Lee and Worthy, 2012; Gorscak et al., 2014; Herrera and Dávalos, 2016; Lund et al., 2016; Sallam and Seifert, 2016; Turner et al., 2017; Argue et al., 2017).

We summarize the results in an “allcompat” summary tree that includes clades with both high and low support. In a strict consensus tree, a summary method for trees recovered through maximum parsimony analysis, clades resolved in all most parsimonious trees (MPTs) are illustrated, even if post-hoc support metrics reveal the clades have weak support. So too, an “allcompat” tree may reveal low posterior probability support for some clades, but these clades are not collapsed because the “allcompat” arrangement shows the most common arrangement of taxa at any given point in the tree. Conclusions drawn from weakly supported clades resolved in the Bayesian consensus tree should be treated cautiously, just as weakly supported clades in a strict consensus tree should be treated cautiously.

In this study, we used MrBayes 3.2.3 (Ronquist et al., 2012) to analyze the character-taxon matrix input file included as Appendix 4. The M_k character model was used for morphological data, the data type was set to “standard” and the coding set “variable”. The analysis was run over 10 x 10⁶ generations with two runs performed simultaneously with four Markov chains. Three chains were heated (temp = 0.02) and the generations sampled every 1000 generations. The first 25% were discarded as part of the burn in period. Convergence was evaluated based on the effective sample size and average standard deviation of split frequencies for the final generation.

Impact of Deciduous Dental Characters on Phylogenetic Inferences

This analysis of hyaenodont relationships inferred using a Bayesian phylogenetic analysis incorporating deciduous dental characters is shown in Figure 12. It is summarized as an “allcompat” (majority-rule plus compatible groups)

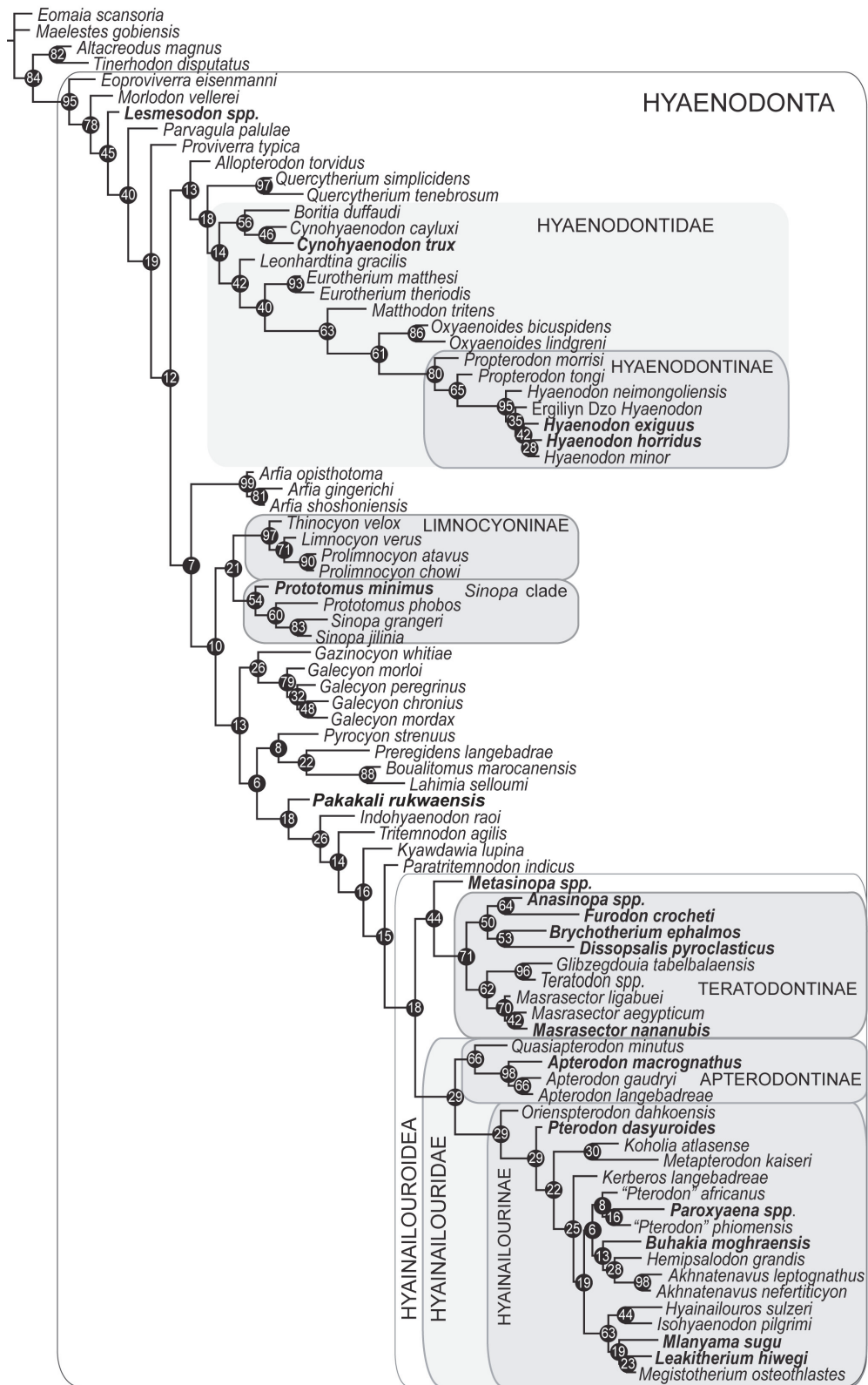


FIGURE 12. Results of the phylogenetic analysis of Hyaenodonta character-taxon matrix including deciduous dental characters. Results are visualized as an “allcompat” (majority rule plus compatible groups) consensus tree. Posterior probabilities (PP) are placed over each node. Bold taxa are scored for deciduous dental characters. Major, named clades recovered or discussed in this analysis and recovered in other analyses are illustrated.

topology with posterior probabilities (PP) shown over the relevant node (“allcompat” tree with additional statistics included as Appendix 5). OTUs that have been scored for deciduous characters are indicated in bold, italicized font. Together with the Borths and Stevens (2017) analysis, this study documents the utility of deciduous dental characters in assessing phylogenetic relationships across hyaenodonts, significantly expanding upon ontogenetic information previously available for just *Hyaenodon* (Bastl and Nagel, 2013). Recent work on hyaenodont systematics has improved sampling for Afro-Arabian OTUs (Borths et al., 2016), placing into context these descriptions of deciduous dentition from a broader sample of Afro-Arabian hyaenodonts.

Description of Phylogenetic Results

As in recent analyses (Borths et al., 2016; Borths and Seiffert, 2017; Borths and Stevens, 2017), our phylogenetic results suggest that the base of the hyaenodont radiation is joined by a sister clade composed of *Altacreodus* and *Tinerhodon*. These taxa have strong support as sister lineages (PP = 0.82) and the clade has strong support (PP = 0.84) as the sister clade of Hyaenodonta.

The earliest-diverging hyaenodont lineage in our study is *Eoproviverra*, diverging from a stem composed of European taxa. Along the hyaenodont stem is *Lesmesodon*, notably a taxon known almost exclusively from specimens that retain deciduous dentition. *Proviverra* is retrieved as the sister taxon of a clade that includes both hyaenodont lineages containing hypercarnivorous taxa: Hyaenodontidae and Hyainailouroidea. The clade that includes Hyaenodontidae incorporates three OTUs with referred deciduous dentition: *Cynohyaenodon trux*, *Hyaenodon exiguus*, and *Hyaenodon horridus*. *C. trux* forms a weakly supported clade with *Cynohyaenodon cayluxi* (PP = 0.46). *H. exiguus* and *H. horridus* are nested within Hyaenodontinae (PP = 0.80) in the clade that includes all other *Hyaenodon* (PP = 0.95) species.

The clade that includes Hyainailouroidea and all Afro-Arabian hyaenodonts is sister to the clade that includes Hyaenodontidae. *Pakakali* is resolved along the stem supporting Hyainailouroidea (PP = 0.18), though it should be noted this taxon is only known from dP³. Hyainailouroidea, the clade that includes Teratodontinae, Apterodontinae, and Hyainailourinae, is weakly supported (PP = 0.18). Within Hyainailouroidea, *Metasinopa* is weakly supported (PP = 0.44) as the sister-taxon of Terat-

odontinae. Teratodontinae is moderately supported as a clade (PP = 0.71). The group formed by *Metasinopa* and Teratodontinae includes several OTUs known from deciduous dental morphology including: *Metasinopa*, *Anasinopa*, *Furodon*, *Brychotherium*, and *Masrasector nananubis*. *Anasinopa* and *Furodon* are moderately supported in this analysis as sister-taxa (PP = 0.64) and weakly supported (PP = 0.50) as part of the same clade as *Brychotherium* and *Dissopsalis*. *Masrasector nananubis* is recovered within the strongly supported *Masrasector* clade (PP = 0.70).

Hyainailouridae includes the moderately supported clade Apterodontinae (PP = 0.66) and the weakly supported clade Hyainailourinae (PP = 0.29). Within Apterodontinae *Apterodon macrogathus* is associated with deciduous dentition and has strong support within the clade *Apterodon*. Within Hyainailourinae, here resolved with *Orienspteron* as the sister lineage of all other hyainailourines, several OTUs are known from deciduous dental morphology: *Pterodon dasyuroides*, *Buhakia moghraensis*, *Paroxyaena*, *Mlanyama sugu*, and *Leakitherium*. *Pterodon dasyuroides* is weakly supported (PP = 0.29) as the sister taxon of all more deeply nested hyainailourines. “*Pterodon*” *africanus* is the sister taxon of a very weakly supported clade (PP = 0.08) that includes *Paroxyaena* and “*Pterodon*” *phiomensis* (PP = 0.16). The *Paroxyaena* + “*Pterodon*” clade is weakly supported (PP = 0.06) as the sister clade of a clade that includes *Buhakia*, *Hemipsalodon* and *Akhnatenuvus*. A more robustly supported Miocene hyainailourine clade (PP = 0.63) is the sister clade of the *Paroxyaena* + *Buhakia* clade. The Miocene hyainailourine clade includes *Hyainailouros sulzeri*, *Isohyaenodon pilgrimi*, *Mlanyama sugu*, *Megistotherium* and *Leakitherium hiwegi*. In this analysis *Leakitherium* is weakly resolved (PP = 0.23) as the sister taxon of *Megistotherium*.

Effect of Deciduous Dental Characters on Hyainailouroid Relationships

With the specimens described here, we can now advocate for the use of deciduous dental characters in the reconstruction of systematic relationships among Afro-Arabian hyainailouroids. The inclusion of deciduous characters might be expected to have a confounding effect on phylogenetic resolution. Deciduous teeth have been hypothesized to retain plesiomorphic characters (Peterkova et al., 2006; Zack, 2012), hence their patchy inclusion might undermine recovery of the structure of phylogenetic relationships established

with adult dental characters. For this reason, we tested the stability of hyaenodont relationships when dental characters were incorporated into the analysis and assessed whether deciduous dentition could be used to build phylogenetic hypotheses, or to make apomorphy-based diagnoses. This is especially important for taxa like *Leakitherium*, *Paroxyaena pavlovi*, *Lesmesodon*, *Buhakia*, and *Pakakali* that are known primarily from deciduous dental material.

Overall, the results of the Bayesian phylogenetic inference including deciduous materials are broadly congruent with the results of the standard Bayesian analysis presented by Borths and Seiffert (2017) for strictly permanent dentition. In particular, taxa retrieved in Hyainailourinae, Apterodontinae, Teratodontinae, and Hyaenodontidae by Borths and Seiffert (2017) were retrieved in similar positions in this study. A difference between the Borths and Seiffert (2017) topology and the present study is the support resolved at the nodes supporting Hyainailouroidea, which are generally weaker when deciduous dental characters and accompanying missing data for many OTUs are included. In both studies, the most likely topologies are similar, but the support for nodes along the stem of Hyainailouroidea and supporting Teratodontinae + Hyainailouridae are weaker. Nonetheless, including deciduous dentition makes it possible to include taxa known primarily from deciduous materials (e.g., *Lesmesodon* or *Pakakali*). With the recovery and description of additional deciduous and adult specimens, resolution and support can be expected to improve along with the application of different phylogenetic methods, such as Bayesian “tip-dating” analysis (Beck and Lee, 2014).

RECONSTRUCTING DENTAL ERUPTION SEQUENCE AND IMPLICATIONS

Dental Eruption Assessment

To reconstruct the order of dental eruption in Hyainailouroidea, we studied multiple isolated specimens in different phases of development. We determined the order of premolar and molar eruption by examining relative tooth wear on adult and deciduous dentition and by examining specimens with tooth germs preserved in the crypt that could be μ -CT scanned at Duke University. Tooth germs in a more advanced stage of development than another germ preserved in the same specimen are considered likely to erupt before the less developmentally advanced germ. This method of identifying an eruption sequence from multiple individuals

follows the efforts of Slaughter et al. (1974), Smith (2000), Anders et al. (2011), Zack (2012), and Bastl and Nagel (2013).

Dental Eruption Sequence in Hyainailouroidea Compared with Other Hyaenodonts

A number of studies of mammalian evolution have explored the dental eruption sequence as a guide for both phylogenetic and developmental hypotheses (Bryant, 1988, 1990; Smith, 2000; Koufos and de Bonis, 2004; Henderson, 2007; Hughes et al., 2007; Asher and Lehmann, 2008; Asher et al., 2017). Based on the materials described in this study, we can now formulate a hypothesis for the order of dental eruption and replacement in Afro-Arabian hyainailouroids. The dental eruption sequence of hyainailouroids can then be compared with the eruption sequences of carnivorous mammals with better known developmental histories (Table 3). Note that there is variation in the dental eruption sequence within different clades of mammals (e.g., Henderson, 2007; Monson and Hlusko, 2016; Asher et al., 2017), and the eruption sequences of different clades of hyaenodonts may emerge as highly variable as more data are collected using scans of the internal anatomy of dentally immature specimens.

For the upper dentition, Borths et al. (2016) described a specimen of the teratodontine *Brychotherium* (DPC 17627) that preserved a fully erupted P⁴ on the right side and a worn dP⁴ on the left side, evidence that DPC 17627 died during the developmental interval when dP⁴ is replaced by its adult counterpart. On the left side, distal to dP⁴, are M¹, M², and M³, evidence that all molars were present before the eruption of P⁴. Unfortunately this specimen does not preserve dP³, P³, or the germ of P³, making it difficult to determine if P³ erupted before P⁴, coincident with the eruption of P⁴ or after P⁴. KNM-RU 15182 (Figure 3) is a maxillary fragment of the hyainailourine *Leakitherium* that preserves P⁴ in the crypt above the roots of dP⁴. In this specimen, the crown of dP³ is preserved but no evidence of P³ is present in the crypt, indicating that P⁴ may have been more fully developed than P³. In *Masrasector nananubis* (DPC 13837, Figure 7) the developmental sequence is flipped, with P³ more fully developed than P⁴. This difference may indicate some variability in the eruption of these premolars in hyainailouroids. No specimens included in this study preserve the upper canines or incisors and dP² is only known from a specimen of *Anasinopa* (KNM-RU 2385), which does not preserve the

TABLE 3. Dental eruption sequences of Hyaenodonta and Ferae. Upper and lower eruption sequences are separated for this study because no hyainailouroid specimen directly reveals the relationship between the timing of eruption in the upper and lower dentition. Sequence reads from left to right with m-dashes identifying subsequent events. Tooth positions contained in parentheses are unknown. Tooth positions with an asterisk are variable within the group. Note that taxa listed in “Group” are not all the same taxonomic level.

Group	Eruption of Upper dentition	Eruption of lower dentition	Reference
Hyainailouroidea synthesis	M ¹ – M ² –M ³ –P ⁴ or P ³ (P ² , C)	M ₁ –M ₂ –P ₂ –P ₃ –M ₃ –P ₄ –C	This study
<i>Apterodon macrognathus</i>		M ₁ –M ₂	This study
<i>Masrasector nananubis</i>	M ¹ –?–?–P ³ –P ⁴	M ₁ –M ₂ –P ₂ –P ₃ –M ₃ –P ₄ –C	This study
<i>Metasinopa</i>		M ₁ –M ₂ –P ₂ –P ₃ –M ₃ –P ₄ –C	This study
<i>Brychotherium ephalmos</i>	M ¹ – M ² –M ³ –P ⁴		This study
<i>Leakitherium hiwegi</i>	?P ⁴ –P ³		This study
North American <i>Hyaenodon</i>	M ¹ – I– P ² – P ⁴ – M ² – P ³ – C	M ₁ –M ₂ –I–P ₂ –P ₄ –M ₃ –P ₃ –C	Bastl and Nagel, 2013
European <i>Hyaenodon</i>	M ¹ – P ¹ – I– P ² – P ⁴ – M ² – P ³ – C	M ₁ –P ₁ –M ₂ –I–P ₂ –C, P ₃ , M ₃ –P ₄	Bastl and Nagel, 2013
<i>Lesmesodon</i>	I–P ¹ –M ¹ –M ² – C– P ²	I–P ₁ –M ₁ –M ₂ –C–P ₂	Morlo and Habersetzer, 1999
<i>Oxyaena woutersi</i>		M ₁ –P ₄ –P ₂ –P ₃ (M ₂)	Solé et al., 2011
<i>Didymictis protenus</i>	M ¹ – P ² /P ³ /P ⁴	P ₂ /M ₁ /M ₂ –P ₃ /P ₄	Zack, 2012
Viverridae	M ¹ – P ⁴ – P ² *– P ³ – M ² *	M ₁ –M ₂ –P ₂ *–P ₃ –P ₄	Slaughter et al., 1974
Felidae	P ² / M ¹ – P ⁴ – P ³	M ₁ –P ₄ –P ₃	Slaughter et al., 1974
Mustelidae	M ¹ – P ⁴ – P ² – P ³	M ₁ –M ₂ –P ₂ *–P ₃ –P ₄	Slaughter et al., 1974
Canidae	M ¹ – M ² – P ⁴ – P ² – P ³	M ₁ /M ₂ –M ₃ *–P ₂ *–P ₄ –P ₃	Slaughter et al., 1974

relationship between P² eruption and molar eruption, leaving the timing of the replacement of these teeth in hyainailouroids unresolved. Based on this information, the order of upper dental eruption in hyainailouroids is:

$$M^1-M^2-M^3-P^3 \text{ or } P^4 \text{ (P}^2, \text{ C, I eruption unresolved)}$$

Equation 1

The eruption sequence for the lower dentition of Hyainailouroidea is better known and can be inferred particularly from specimens of *Masrasector nananubis* (DPC 18276, Figure 8; DPC 10358, Figure 9), *Metasinopa* (DPC 4544, Figure 11), and *Buhakia* (DPC 8994; Morlo et al., 2007, figure 2). In *Masrasector* and *Metasinopa* M₂ erupted before the premolars and canine. In both taxa P₂ is the most developed premolar, evidence it was the first permanent premolar to erupt, followed by P₃. The dentary specimen of *Metasinopa* (DPC 4544, Figure 11) preserves M₃ near the alveolar margin and more developed than P₄. Of the permanent dentition preserved in DPC 4544, the canine is the least developed, likely making it the last permanent

tooth in the dentary. Based on this information the order of lower dental eruption in hyainailouroids is:

$$M_1-M_2-P_2-P_3-M_3-P_4-C$$

Equation 2

Morlo et al. (2007) described the left dentary of *Buhakia moghraensis*, and they identified the preserved crowns as dP₄, M₁, and M₂. They also interpreted alveoli on the specimen as evidence of dP₃ and dP₂. We concur with this interpretation, as M₂ had recently erupted in the holotype of *Buhakia* and DPC 4544 (*Metasinopa*) shows dP₂ was not replaced until M₂ was fully erupted. Solé et al. (2016) also identified a dentary fragment of the Afro-Arabian hyaenodont, *Parvavorodon* (CBI-1-63), with the alveoli of dP₃, the crowns of dP₄, and M₁, and the alveoli of M₂. Based on a CT-scan of the specimen, they determined the germs of P₃ and P₄ had not yet formed in the crypts below dP₃ and dP₄ despite the presence of M₂. This suggests *Parvavorodon* differs from *Masrasector nananubis* developmentally as one specimen of *Masrasector* (DPC 18276, Figure 8) preserves the germs of P₂,

P₃, and M₂ each developing in their crypts contemporaneously.

In *Hyaenodon*, Bastl and Nagel (2013) reconstructed North American *Hyaenodon* with the upper dental eruption sequence M¹–I–P²–P⁴–M²–P³–C and lower dental eruption sequence M₁–M₂–I–P₂–P₄–M₃–P₃–C. European *Hyaenodon* is reconstructed with the upper eruption sequence M¹–P¹–I–P²–P⁴–M²–P³–C and M₁–P₁–M₂–I–P₂–C, P₃, M₃–P₄. The lower eruption sequence of hyainailouroids is most like the lower eruption sequence of European *Hyaenodon*, with M₃ erupting before the emergence of P₄. The upper eruption sequence of hyainailouroids differs from the reconstructed sequence in both European and North American *Hyaenodon*. In *Hyaenodon*, P⁴ emerges before M². In *Brychotherium* M² is already erupted when P⁴ is being replaced and M³ is emerging.

With multiple specimens of *Lesmesodon*, Morlo, and Habersetzer (1999) reconstructed the partial eruption sequence of this Eocene hyaenodont known almost exclusively from dentally immature individuals found in the Messel Pit in Germany. Like hyainailouroids, *Lesmesodon* replaced dP₂ after the eruption of M₁ and M₂. *Lesmesodon* is consistently resolved as part of an early-diverging lineage (Borths et al., 2016; Borths and Seiffert, 2017) with other European mesocarnivorous hyaenodonts that have been allied with “Proviverrinae” (Solé et al., 2014). This phylogenetic position supports the *Lesmesodon* eruption sequence (P₂ erupted after M₂) as the ancestral condition in Hyaenodonta.

Dental Eruption Sequence of Hyaenodonta Compared with Other Carnivorous Mammals

Traditionally, Hyaenodonta is allied with Oxyaenidae in “Creodonta” and “Creodonta” is placed within Ferae, the clade that includes Pholidota and Carnivora (Rose, 2006). This phylogenetic hypothesis collects most placental mammals with specialized carnassials in the same clade (Spaulding et al., 2009; O’Leary et al., 2013; Halliday et al., 2015). As summarized by Rana et al. (2015) and Borths et al. (2016), these relationships—including the sister-clade relationship between hyaenodonts and oxyaenids—require further phylogenetic testing.

The dental eruption sequence of *Oxyaena woutersi* was partially reconstructed by Solé et al.

(2011) based on MNHN QNY2-2527 as M₁–P₄–P₂–P₃. The specimen preserves neither M₂, nor its alveoli, making it difficult to determine whether the premolars were replaced before or after the terminal molar erupted. Regardless, the eruption of P₄ before the eruption of P₂ and P₃ is different from all hyaenodont eruption sequences known. This difference may support the hypothesis that hyaenodonts and oxyaenids converged on dentition specialized for carnivory, and may not be sister clades (Polly, 1996) in Ferae nor form a monophyletic Creodonta.

The order of dental eruption differs within Carnivora. Slaughter et al. (1974) observed that Mustelidae and Viverridae, two distantly related carnivoran clades that contain mesocarnivorous taxa, share eruption sequences: M¹–P⁴–P²–P³–M²; M₁–M₂–P₂–P₃–P₄. Slaughter et al. (1974) noted that the eruption of P², P₂, and M² (when present) is variable but in both groups, P₃ is replaced before P₄, a pattern also observed by Bastl and Nagel (2013) in *Hyaenodon* and in this study in *Masrasector* and *Metasinopa*.

In contrast to Mustelidae and Viverridae, in Canidae and Felidae P₄ erupts before P₃. Slaughter et al. (1974) suggested this may represent an adaptation in two distantly related clades to preserve the deciduous carnassial formed between dP³ and dP₄ until after the full eruption and occlusion of P⁴ and M₁ has taken place. This developmental convergence highlights the importance of a functioning carnassial in carnivorans. A key morphological difference between Carnivora and Hyaenodonta is that in Carnivora, an individual only develops two carnassials through the course of its lifetime. In hyaenodonts, an individual develops four: dP³/dP₄, P⁴/M₁, M¹/M₂, and M²/M₃. European *Hyaenodon* follows the hypercarnivorous pattern by delaying the replacement of the deciduous carnassial until the final carnassial complex is formed between M²/M₃, suggesting that even in a lineage with multiple carnassials, there was selective pressure to preserve the deciduous carnassial as long as possible. Similarities in the dental eruption sequence do not refute a possible relationship between Carnivora and Hyaenodonta. Significant differences between the clades, however, do raise the question of how in each case the dental eruption sequence interfaces with the development of the rest of the animal.

What Does the Timing of Tooth Eruption Tell Us about Hyainailouroids?

In many carnivorans it only takes up to one year for the adult dentition to fully erupt (Miles and Grigson, 1990). In contrast, Bastl and Nagel (2013) demonstrated through enamel studies that *Hyae-nodon* took between three and four years to develop its adult dentition, implying either that hyaenodonts developed more slowly overall than carnivorans, or that dental replacement was decoupled from the skeletal and cranial development such that dentally immature hyaenodont individuals may have been reproductively mature.

The “developmental decoupling” hypothesis is supported by a cranial specimen of *Paroxyaena pavlovi* described by Lavrov (2007). Lavrov (2007) noted that the specimen retains dP³ and dP⁴, but already has the well-sutured cranial vault of a mature individual. Notably, *Paroxyaena* retained a functional dP³/dP₄ carnassial complex at an adult body size. *Brychotherium* also exhibits an adult-sized rostrum with dP⁴ still in the maxilla as M³ erupted. This extended dental developmental interval would have allowed these hyainailouroids to wear the deciduous carnassial for up to three extra years, a significantly longer interval compared with carnivorans. When P³ and P₄ finally erupted, they erupted into a fully mature dentary and were spared from years of accumulated wear, wear that is preserved on the dP₄ of *Metasinopa* (DPC 4544) and dP³ of *Pakakali* (Borths and Stevens, 2017).

Modern carnivorans can break their teeth while capturing and processing their prey (Van Valkenburgh, 1988; Binder and Van Valkenburgh, 2010), evidence that risk of damage to the permanent dentition may act as a selective pressure upon tooth morphology and replacement. Exceeding the safety factors that lead to tooth breakage is not common (Van Valkenburgh, 1988), indicating morphological and behavioral adaptations tend to prevent it, but the abrasion of teeth is less preventable on an individual level in carnivorans and is so constant a pressure that the metric can be used to age carnivorans in the field (e.g., White and Belant, 2016; Chevallier et al., 2017). Binder and Van Valkenburgh (2000) observed that in hyenas, there is a shift in tooth use with age from mesial deciduous premolars to distal adult premolars. Binder and Van Valkenburgh (2000) hypothesized this shift could serve to protect the single carnassial pair. Ultimately, these studies demonstrate that shearing crest preservation may be a selective pressure for carnivorous mammals. By delaying the replace-

ment of the deciduous carnassial and erupting permanent carnassial pairs while the deciduous carnassial was active, hyaenodonts preserved their ability to access vertebrate prey throughout their lives, guarding against breakage and excessive wear.

One strange aspect of the hyaenodont fossil record is the abundance of dentally immature specimens. Every specimen of *Lesmesodon* collected from Messel preserves deciduous dentition. Of the three known maxilla fragments of *Leakitherium*, two preserve dP³ and dP⁴. The holotype of *Mlanyama sugu* preserves dP₄. We suggest that if dental development occurred over a longer temporal duration in hyaenodonts than in, for example, carnivores, it would be increasingly likely for immature individuals to be preserved in the fossil record, and this might explain a relatively high number of specimens preserving deciduous teeth in this clade.

The early ontogeny of mammals is not generally the phenotype used to interpret the ecological position of a taxon. In carnivorans, dentally immature individuals are usually less than a year old, hence it is justifiable to focus on a dentally mature individual as the phenotype that natural selection is primarily acting upon. This is defined by Anders et al. (2011) as individual dental age stage (IDAS) 3—adult. But in hyaenodonts, the phenotype interacting with the environment for multiple years was IDAS 2 (juvenile). Delayed eruption of adult dentition has also been noted by Asher and Lehmann (2008) and Asher et al. (2017) for the clade Afrotheria. Although interesting, any implications of that similarity are beyond the scope of this study. The Pleistocene bovid *Myotragus balearicus* (Jordana and Köhler, 2011) also extended the period of dental development relative to its body size, a shift the authors suggest may have been related to the resource-poor island habitat occupied by *M. balearicus*. Perhaps shifts in hyainailouroid life history and dental development reflect changes in resource availability related to environmental changes in the Paleogene-Neogene of Afro-Arabia.

To date, most ecological comparisons between carnivorans and hyaenodonts have been based upon the adult phenotypes of both groups. This is understandable, as both share similar dental eruption sequences, both have specialized carnassials, and both exhibit postcranial adaptations for carnivory. Yet hyainailouroids appear to have employed a different ontogenetic timing strategy from Carnivora, hence future hypotheses to explain

the success of Carnivora and the extinction of Hyaenodonta should address developmental differences between the two most diverse carnivorous mammalian lineages of the Cenozoic. Indeed, additional research is needed to account for life history metrics such as the rate of tooth growth (Smuts et al., 1978), the development of the pulp cavity (Meachen-Samuels and Binder, 2010), and the inference of growth rates from long bones (Kolb et al., 2015) as potential sources of data in exploring the differences between carnivoran and hyaenodont ontogeny.

CONCLUSIONS

Deciduous dental morphology has been underutilized in the larger effort to understand hyaenodont biology. In this study, we describe specimens referred to six different species of Hyainailouroidea, the hyaenodont clade that contains the majority of Afro-Arabian hyaenodonts. We demonstrate that phylogenetically informative character information is preserved in deciduous dental morphology, and that these characters can be used to explore hyaenodont relationships. Based on the specimens described herein, we reconstruct the dental eruption sequence of hyainailourid hyaenodonts. The dental eruption sequence is a rich source of additional systematic insight in the ongoing effort to understand the placental tree of life. Correlating the dental eruption sequence of Hyainailouroidea with cranial development, we suggest that hyaenodonts in Afro-Arabia and in Eurasia exhibited an extended period of dental eruption. Delayed dental replacement in hyaenodonts allowed these carnivorous mammals to spread carnassial wear across the tooth row, and freed hyaenodonts from dependence on a single, functional permanent pair carnassial. In contrast, Carnivora quickly erupts the adult dentition and is limited to one pair of carnassials on each side of the mouth that must survive throughout the individual's life. Understanding the deciduous dentition of hyaenodonts is essential for understanding both the higher-order relationships of the group, and for understanding the biology of this widespread and morphologically diverse radiation of carnivorous mammals.

ACKNOWLEDGMENTS

We dedicate this project to the memory of Gregg F. Gunnell: mentor, friend, and fossil hunter. We thank the Egyptian Mineral Resources Authority and the Egyptian Geological Museum for facilitating fieldwork in the Fayum area, P. Chatrath for managing fieldwork, and multiple Fayum field crews for the efforts in excavating the Fayum area. We also thank the National Commission for Science, Technology and Innovation in Kenya and the National Museums of Kenya for facilitating specimen access in Kenya. Scanning assistance at Duke University was provided by H. Sallam and S. Heritage and imaging assistance at the University of Southern California was provided by B. Patel and E. Seiffert. Imaging assistance at Ohio University was provided by K. Brock, J. Piurowski, B. Sanders, S. Travis, and S. Aftabizadeh. We thank the many curators and collections managers who have coordinated access to their collections including C. Argot and G. Billet (Muséum National d'Histoire Naturelle, Paris), M. Brett-Surman (National Museum of Natural History, Washington, D.C), P. Brewer (Natural History Museum, London), L. Costeur (Naturhistorisches Museum, Basel), J. Chupasko and J. Cundiff (Museum of Comparative Zoology, Cambridge), J. Galkin (AMNH), G. Gunnell (DPC), M. Hellmund (Geiseltal Museum, Halle), J. Hooker (Natural History Museum, London), A. Lavrov (Paleontological Institute, Moscow), E. Mbuu, F. Manthi, M. Muungu, and F. Ndiritu (KNM), C. Norris (Yale Peabody Museum, New Haven), S. Pierce (Museum of Comparative Zoology, Cambridge), T. Smith (Institut royal des Sciences naturelles de Belgique, Brussels), S. Schaal (SMF), F. Solé (Institut royal des Sciences naturelles de Belgique, Brussels), B. Sanders (University of Michigan, Ann Arbor), G. Rössner (BSPG), A. Sileem (CGM), A. Vogel (Naturmuseum Senckenberg, Frankfurt am Main), E. Westwig (AMNH), N. Xijun (Institute for Vertebrate Paleontology and Paleoanthropology, Beijing), and R. Ziegler (SMNS) for specimen access. Funding by: The Explorers Club, the Society for Integrative and Comparative Biology, and the National Science Foundation (BCS- 1638796; DEB-1311354; DBI- 1612062).

REFERENCES

- Anders, U., von Koenigswald, W., Ruf, I., and Smith, B.H. 2011. Generalized individual dental age stages for fossil and extant placental mammals. *Paläontologische Zeitschrift*, 85:321-339. <https://doi.org/10.1007/s12542-011-0098-9>

- Andrews, C.W. 1904. Further notes on the mammals of the Eocene of Egypt. *Geological Magazine*, 5:109-115 and 157-162. <https://doi.org/10.1017/S001675680012343X>
- Andrews, C.W. 1906. *A Descriptive Catalogue of the Tertiary Vertebrata of the Fayum, Egypt*. British Museum of Natural History, London. <https://doi.org/10.5962/bhl.title.55134>
- Argue, D., Groves, C.P., Lee, M.S.Y., and Jungers, W.L. 2017. The affinities of *Homo floresiensis* based on phylogenetic analyses of cranial, dental, and postcranial characters. *Journal of Human Evolution*. <https://doi.org/10.1016/j.jhevol.2017.02.006>
- Asher, R.J., Gunnell, G.F., Seiffert, E.R., Pattinson, D., Tabuce, R., Hautier, L., and Sallam, H.M. 2017. Dental eruption and growth in Hyracoidea (Mammalia, Afrotheria). *Journal of Vertebrate Paleontology*, 37:e1317638. <https://doi.org/10.1080/02724634.2017.1317638>
- Asher, R.J. and Lehmann, T. 2008. Dental eruption in afrotherian mammals. *BMC Biology*, 6(1):14. <https://doi.org/10.1186/1741-7007-6-14>
- Barry, J.C. 1988. *Dissopsalis*, a middle and late Miocene proviverrine creodont (Mammalia) from Pakistan and Kenya. *Journal of Vertebrate Paleontology*, 8:25-45. <https://doi.org/10.1080/02724634.1988.10011682>
- Bastl, K., Morlo, M., Nagel, D., and Heizmann, E. 2011. Differences in the tooth eruption sequence in *Hyaenodon* ('Creodonta': Mammalia) and implications for the systematics of the genus. *Journal of Vertebrate Paleontology*, 31:181-192. <https://doi.org/10.1080/02724634.2011.540052>
- Bastl, K. and Nagel, D. 2013. First evidence of the tooth eruption sequence of the upper jaw in *Hyaenodon* (Hyaenodontidae, Mammalia) and new information on the ontogenetic development of its dentition. *Paläontologische Zeitschrift*, 88:481-494. <https://doi.org/10.1007/s12542-013-0207-z>
- Bastl, K., Nagel, D., and Peigné, S. 2014. Milk tooth morphology of small-sized *Hyaenodon* (Hyaenodontidae, Mammalia) from the European Oligocene—evidence of a *Hyaenodon* lineage in Europe. *Palaeontographica, Abt A: Palaeozoology–Stratigraphy*, 303:61-84. <https://doi.org/10.1127/pala/303/2014/61>
- Beck, R.M.D. and Lee, M.S.Y. 2014. Ancient dates or accelerated rates? Morphological clocks and the antiquity of placental mammals. *Proceedings of the Royal Society B: Biological Sciences*, 281(1793):20141278. <https://doi.org/10.1098/rspb.2014.1278>
- Binder, W.J. and Van Valkenburgh, B. 2000. Development of bite strength and feeding behaviour in juvenile spotted hyenas (*Crocuta crocuta*). *Journal of Zoology*, 252:273-283. <https://doi.org/10.1111/j.1469-7998.2000.tb00622.x>
- Binder, W.J. and Van Valkenburgh, B. 2010. A comparison of tooth wear and breakage in Rancho La Brea sabertooth cats and dire wolves across time. *Journal of Vertebrate Paleontology*, 30:255-261. <https://doi.org/10.1080/02724630903413016>
- Borths, M.R., Holroyd, P.A., and Seiffert, E.R. 2016. Hyainailourinae and Teratodontinae cranial material from the late Eocene of Egypt and the application of parsimony and Bayesian methods to the phylogeny and biogeography of Hyaenodonta (Placentalia, Mammalia). *PeerJ*, 4:e2639. <http://doi.org/10.7717/peerj.2639>
- Borths, M.R. and Seiffert, E.R. 2017. Craniodental and humeral morphology of a new species of *Masrasector* (Teratodontinae, Hyaenodonta, Placentalia) from the late Eocene of Egypt and locomotor diversity in hyaenodonts. *PLOS ONE*, 12(4):e0173527. <https://doi.org/10.1371/journal.pone.0173527>
- Borths, M.R. and Stevens, N.J. 2017. The first hyaenodont from the late Oligocene Nsungwe Formation of Tanzania: insights into the Paleogene-Neogene carnivore transition. *PLOS ONE*, 12(10):e0185301. <https://doi.org/10.1371/journal.pone.0185301>
- Bryant, H.N. 1988. Delayed eruption of the deciduous upper canine in the sabertoothed carnivore *Barbourofelis lovei* (Carnivora, Nimravidae). *Journal of Vertebrate Paleontology*, 8:295-306. <https://doi.org/10.1080/02724634.1988.10011712>
- Bryant, H.N. 1990. Implications of the dental eruption sequence in *Barbourofelis* (Carnivora, Nimravidae) for the function of upper canines and the duration of parental care in sabertoothed carnivores. *Journal of Zoology*, 222:585-590. <https://doi.org/10.1111/j.1469-7998.1990.tb06015.x>
- Chevallier, C., Gauthier, G., and Berteaux, D. 2017. Age estimation of live arctic foxes *Vulpes lagopus* based on teeth condition. *Wildlife Biology*, 17:wlb.00304. <https://doi.org/10.2981/wlb.00304>

- Ciancio, M.R., Castro, M.C., Galliari, F.C., Carlini, A.A., and Asher, R.J. 2012. Evolutionary implications of dental eruption in *Dasypus* (Xenarthra). *Journal of Mammalian Evolution*, 19:1-8. <https://doi.org/10.1007/s10914-011-9177-7>
- Codron, D., Carbone, C., and Clauss, M. 2013. Ecological interactions in dinosaur communities: influences of small offspring and complex ontogenetic life histories. *PLoS ONE*, 8(10):e77110. <https://doi.org/10.1371/journal.pone.0077110>
- Coutinho, S., Buschang, P.H., and Miranda, F. 1993. Relationships between mandibular canine calcification stages and skeletal maturity. *American Journal of Orthodontics and Dentofacial Orthopedics*, 104:262-268. [https://doi.org/10.1016/S0889-5406\(05\)81728-7](https://doi.org/10.1016/S0889-5406(05)81728-7)
- Crochet, J.-Y., Thomas, H., Roger, J., and Al-Sulaimani, S. 1990. Première découverte d'un créodonte dans la péninsule Arabique: *Masrasektor ligabuei* nov. sp. (Oligocène inférieur de Taqah, Formation d'Ashawq, Sultanat d'Oman). *Comptes rendus de l'Académie des sciences, Paris, Série II*, 311:1455-1460.
- de Queiroz, K. 1985. The ontogenetic method for determining character polarity and its relevance to phylogenetic systematics. *Systematic Biology*, 34:280-299. <https://doi.org/10.1093/sysbio/34.3.280>
- Finarelli, J.A. and Flynn, J.J. 2009. Brain-size evolution and sociality in Carnivora. *Proceedings of the National Academy of Sciences, USA*, 106:9345-9349. <https://doi.org/10.1073/pnas.0901780106>
- Fink, W.L. 1982. The conceptual relationship between ontogeny and phylogeny. *Paleobiology*, 8:254-264. <https://doi.org/10.1017/S0094837300006977>
- Fischer, P. 1880. Note sur un nouveau genre de mammifère fossile (*Apterodon gaudryi*) des Phosphorites du Quercy. *Bulletin de la Société Géologique de France*, 8:288-290.
- Gorscak, E., O'Connor, P.M., Stevens, N.J., and Roberts, E.M. 2014. The basal titanosaurian *Rukwatitan bisepultus* (Dinosauria: Sauropoda) from the middle Cretaceous Galula Formation, Rukwa Rift Basin, southwestern Tanzania. *Journal of Vertebrate Paleontology*, 34:1133-1154. <https://doi.org/10.1080/02724634.2014.845568>
- Goswami, A. and Polly, P.D. 2010. The influence of modularity on cranial morphological disparity in Carnivora and Primates. *PLOS ONE*, 5(3):e9517. <https://doi.org/10.1371/journal.pone.0009517>
- Grohé, C., Morlo, M., Chaimanee, Y., Blondel, C., Coster, P., Valentin, X., Salem, M., Bilal, A.A., Jaeger, J.-J., and Brunet, M. 2012. New Apterodontinae (Hyaenodontida) from the Eocene locality of Dur At-Talah (Libya): systematic, paleoecological and phylogenetical implications. *PLOS ONE* 7(11):e49054. <https://doi.org/10.1371/journal.pone.0049054>
- Halliday, T.J.D., Upchurch, P., and Goswami, A. 2015. Resolving the relationships of Paleocene placental mammals. *Biological Reviews*, 92:521-550. <https://doi.org/10.1111/brv.12242>
- Henderson, E. 2007. Platyrrhine dental eruption sequences. *American Journal of Physical Anthropology*, 134:226-239. <https://doi.org/10.1002/ajpa.20658>
- Herrera, J.P. and Dávalos, L.M. 2016. Phylogeny and divergence times of lemurs inferred with recent and ancient fossils in the tree. *Systematic Biology*, 65:772-791. <https://doi.org/10.1093/sysbio/syw035>
- Holroyd, P.A. 1999. New Pterodontinae (Creodonta: Hyaenodontidae) from the late Eocene–early Oligocene Jebel Qatrani Formation, Fayum Province, Egypt. *PaleoBios*, 19(2):1-18.
- Hone, D.W.E., Farke, A.A., and Wedel, M.J. 2016. Ontogeny and the fossil record: what, if anything, is an adult dinosaur? *Biology Letters*, 12: 20150947. <https://doi.org/10.1098/rsbl.2015.0947>
- Hughes, T., Dempsey, P., Richards, L., and Townsend, G. 2000. Genetic analysis of deciduous tooth size in Australian twins. *Archives of Oral Biology*, 45:997-1004. [https://doi.org/10.1016/S0003-9969\(00\)00066-2](https://doi.org/10.1016/S0003-9969(00)00066-2)
- Hughes, T.E., Bockmann, M.R., Seow, K., Gotjamanos, T., Gully, N., Richards, L.C., and Townsend, G.C. 2007. Strong genetic control of emergence of human primary incisors. *Journal of Dental Research*, 86:1160-1165. <https://doi.org/10.1177/154405910708601204>
- Kolb, C., Scheyer, T.M., Veitschegger, K., Forasiepi, A.M., Amson, E., van der Geer, A.A.E., Van den Hoek Ostende, L.W., Hayashi, S., and Sánchez-Villagra, M.R. 2015. Mammalian bone palaeohistology: a survey and new data with emphasis on island forms. *PeerJ*, 3:e1358. <https://doi.org/10.7717/peerj.1358>
- Koufos, G.D. and de Bonis, L. 2004. The deciduous lower dentition of *Ouranopithecus macedoniensis* (Primates, Hominoidea) from the late Miocene deposits of Macedonia,

- Greece. *Journal of Human Evolution*, 46:699-718. <https://doi.org/10.1016/j.jhevol.2004.03.007>
- Lange-Badré, B. and Böhme, M. 2005. *Apterodon intermedius*, sp. nov., a new European creodont mammal from MP22 of Espenhain (Germany). *Annals de Paléontologie*, 91:311-328. <https://doi.org/10.1016/j.annpal.2005.08.001>
- Lavrov, A.V. 2007. A new species of *Paroxyaena* (Hyaenodontidae, Creodonta) from Phosphorites of Quercy, Late Eocene, France. *Paleontological Journal*, 41:298-311. <https://doi.org/10.1134/S0031030107040144>
- Lee, M.S.Y. and Worthy, T.H. 2012. Likelihood reinstates *Archaeopteryx* as a primitive bird. *Biology Letters*, 8:299-303. <https://doi.org/10.1098/rsbl.2011.0884>
- Lewis, M.E. and Morlo, M. 2010. Creodonta, p. 543-560. In Werdelin, L. and Sanders, W. (eds.), *Cenozoic Mammals of Africa*. University of California Press, Berkeley.
- Lindström, J. 1999. Early development and fitness in birds and mammals. *Trends in Ecology and Evolution*, 14:343-348. [https://doi.org/10.1016/S0169-5347\(99\)01639-0](https://doi.org/10.1016/S0169-5347(99)01639-0)
- Linnaeus, C. 1758. *Systema Naturae per regna tria naturae, secundum classes, ordines, genera, species, cum characteribus, differentiis, synonymis, locis*. Editio decima, reformata. Holmiae: Laurentius Salvius. <https://doi.org/10.5962/bhl.title.542>
- Lund, E.K., O'Connor, P.M., Loewen, M.A., and Jinnah, Z.A. 2016. A new centrosaurine ceratopsid, *Machairoceratops cronusi* gen et sp. nov., from the Upper Sand Member of the Wahweap Formation (Middle Campanian), Southern Utah. *PLoS ONE*, 11(5):e0154403. <https://doi.org/10.1371/journal.pone.0154403>
- Meachen-Samuels, J.A. and Binder, W.J. 2010. Sexual dimorphism and ontogenetic growth in the American lion and sabertoothed cat from Rancho La Brea. *Journal of Zoology*, 280:271-279. <https://doi.org/10.1111/j.1469-7998.2009.00659.x>
- Mellett, J.S. 1977. Paleobiology of North American *Hyaenodon* (Mammalia, Creodonta). *Contributions to Vertebrate Evolution*, 1:1-134.
- Miles, A.E.W. and Grigson, C. 1990. *Colyer's Variations and Diseases of the Teeth of Animals*. Cambridge University Press, Cambridge, UK.
- Miller, E.R., Gunnell, G.F., Seiffert, E.R., Sallam, H., and Schwartz, G.T. 2017. Patterns of dental emergence in early anthropoid primates from the Fayum Depression, Egypt. *Historical Biology*, 1-9. <https://doi.org/10.1080/08912963.2017.1294169>
- Monson, T.A. and Hlusko, L.J. 2016. The evolution of dental eruption sequence in artiodactyls. *Journal of Mammalian Evolution*. <https://doi.org/10.1007/s10914-016-9362-9>
- Morales, J., Brewer, P., and Pickford, M. 2010. Carnivores (Creodonta and Carnivora) from the basal middle Miocene of Gebel Zelten, Libya, with a note on a large amphicyonid from the middle Miocene of Ngorora, Kenya. *Bulletin of the Tethys Geological Society, Cairo*, 5:43-54.
- Morales, J., Pickford, M., Fraile, S., Salesa, M.J., and Soria, D. 2007. New carnivoran material (Creodonta, Carnivora and Incertae sedis) from the early Miocene of Napak, Uganda. *Paleontological Research*, 11:71-84. [https://doi.org/10.2517/1342-8144\(2007\)11\[71:NCMCCA\]2.0.CO;2](https://doi.org/10.2517/1342-8144(2007)11[71:NCMCCA]2.0.CO;2)
- Morlo, M. and Habersetzer, J. 1999. The Hyaenodontidae (Creodonta, Mammalia) from the lower middle Eocene (MP 11) of Messel (Germany) with special remarks on new x-ray methods. *Courier Forschungsinstitut Senckenberg*, 216:31-73.
- Morlo, M., Miller, E.R., and El-Barkooky, A.N. 2007. Creodonta and Carnivora from Wadi Moghra, Egypt. *Journal of Vertebrate Paleontology*, 27:145-159. [https://doi.org/10.1671/0272-4634\(2007\)27\[145:CACFWM\]2.0.CO;2](https://doi.org/10.1671/0272-4634(2007)27[145:CACFWM]2.0.CO;2)
- O'Leary, M.A., Bloch, J.I., Flynn, J.J., Gaudin, T.J., Giallombardo, A., Giannini, N.P., Goldberg, S.L., Kraatz, B.P., Luo, Z.-X., Meng, J., Ni, X., Novacek, M.J., Perini, F.A., Randall, Z.S., Rougier, G.W., Sargis, E.J., Silcox, M.T., Simmons, N.B., Spaulding, M., Velazco, P.M., Weksler, M., Wible, J.R., and Cirranello, A.L. 2013. The placental mammal ancestor and the post-K-Pg radiation of placentals. *Science*, 339:662-667. <https://doi.org/10.1126/science.1229237>
- Osborn H.F. 1909. New carnivorous mammals from the Fayum Oligocene, Egypt. *Bulletin of the American Museum of Natural History*, 26:415-424. <http://hdl.handle.net/2246/1452>
- Peterkova, R., Lesot, H., and Peterka, M. 2006. Phylogenetic memory of developing mammalian dentition. *Journal of Experimental Biology (Molecular and Developmental Evolution)*, 306B:234-250. <https://doi.org/10.1002/jez.b.21093>
- Pilgrim, G.E. 1910. Notices of new mammalian genera and species from the Tertiaries of India. *Records of the Geological Survey of India*, 40:63-71.

- Pilgrim, G.E. 1932. The fossil Carnivora of India. *Memoirs of the Geological Survey of India. Palaeontologica Indica*, 18:1-232. <https://doi.org/10.1017/S0016756800096448>
- Polly, P.D. 1996. The skeleton of *Gazinocyon vulpeculus* gen. et comb. nov. and the cladistic relationships of Hyaenodontidae (Eutheria, Mammalia). *Journal of Vertebrate Paleontology*, 16:303-319. <https://doi.org/10.1080/02724634.1996.10011318>
- Rager, L., Hautier, L., Forasiepi, A., Goswami, A., and Sánchez-Villagra, M. R. 2013. Timing of cranial suture closure in placental mammals: phylogenetic patterns, intraspecific variation, and comparison with marsupials. *Journal of Morphology*, 275:125-140. <https://doi.org/10.1002/jmor.20203>
- Rana, R., Kumar, K., Zack, S., Solé, F., Rose, K., Missiaen, K.P., Singh, L., Sahni, A., and Smith, T. 2015. Craniodental and postcranial morphology of *Indohyaenodon raoi* from the early Eocene of India, and its implications for ecology, phylogeny, and biogeography of hyaenodontid mammals. *Journal of Vertebrate Paleontology*. 35:e965308. <https://doi.org/10.1080/02724634.2015.965308>
- Ronquist, F., Teslenko, M., van der Mark, P., Ayres, D.L., Darling, A., Höhna, S., Larget, B., Liu, L., Suchard, M.A., and Huelsenbeck, J.P. 2012. MrBayes 3.2: efficient Bayesian phylogenetic inference and model choice across a large model space. *Systematic Biology*, 61:539-542. <https://doi.org/10.1093/sysbio/sys029>
- Rose, K. 2006. *The Beginning of the Age of Mammals*. Johns Hopkins University Press, Baltimore.
- Ross, C. 1996. Adaptive explanation for the origins of the Anthropoidea (Primates). *American Journal of Primatology*, 40:205-230. [https://doi.org/10.1002/\(SICI\)1098-2345\(1996\)40:3<205::AID-AJP1>3.0.CO;2-1](https://doi.org/10.1002/(SICI)1098-2345(1996)40:3<205::AID-AJP1>3.0.CO;2-1)
- Sallam, H.M. and Seiffert, E.R. 2016. New phiomorph rodents from the latest Eocene of Egypt, and the impact of Bayesian “clock”-based phylogenetic methods on estimates of basal hystricognath relationships and biochronology. *PeerJ*, 4:e1717. <https://doi.org/10.7717/peerj.1717>
- Sánchez-Villagra, M.R. 2010a. Developmental palaeontology in synapsids: the fossil record of ontogeny in mammals and their closest relatives. 20092005 *Proceedings of the Royal Society B*. <https://doi.org/10.1098/rspb.2009.2005>
- Sánchez-Villagra, M.R. 2010b. Suture closure as a paradigm to study late growth in recent and fossil mammals: a case study with giant deer and dwarf deer skulls. *Journal of Vertebrate Paleontology*, 30:1895-1898. <https://doi.org/10.1080/02724634.2010.521218>
- Savage, R.J.G. 1965. Fossil mammals of Africa 19: the Miocene Carnivora of East Africa. *Bulletin of the British Museum of Natural History (Geology)*, 10:239-316. <http://direct.biostor.org/reference/118744>
- Schlosser, M. 1910. Über einige fossil säugetiere aus dem Oligocän von Ägypten. *Zoologischer Anzeiger*, 35:500-508. <https://biodiversitylibrary.org/page/9741941>
- Schneider, C.A., Rasband, W.S., and Eliceiri, K.W. 2012. NIH Image to ImageJ: 25 years of image analysis. *Nature Methods*, 9:671-675. <https://doi.org/10.1038/nmeth.2089>
- Shubin, N.H., Daeschler, E.B., and Jenkins, F.A. 2006. The pectoral fin of *Tiktaalik roseae* and the origin of the tetrapod limb. *Nature*, 440:764-771. <https://doi.org/10.1038/nature04637>
- Simons, E.L. and Gingerich, P.D. 1974. New carnivorous mammals from the Oligocene of Egypt. *Annals of the Geological Survey of Egypt*, 4:157-166.
- Slaughter, B.H., Pine, R.H., and Pine, N.E. 1974. Eruption of cheek teeth in Insectivora and Carnivora. *Journal of Mammalogy*, 55:115-125. <https://doi.org/10.2307/1379261>
- Smith, B.H. 1989. Dental development as a measure of life history in primates. *Evolution*, 43:683-688. <https://doi.org/10.1111/j.1558-5646.1989.tb04266.x>
- Smith, B.H. 2000. Schultz's rule and the evolution of tooth emergence and replacement patterns in primates and ungulates, p. 212-217. In Teaford, M.F., Smith, M.M., and Ferguson, M.W.J. (eds.), *Development, Function and Evolution of Teeth*. Cambridge University Press, Cambridge, U.K.
- Smuts, G.L., Anderson, J.L., and Austin, J.C. 1978. Age determination of the African lion (*Panthera leo*). *Journal of Zoology*, 185:115-146. <https://doi.org/10.1111/j.1469-7998.1978.tb03317.x>
- Solé, F., Amson, E., Borths, M., Vidalenc, D., Morlo, M., and Bastl, K. 2015. A new large hyainailourine from the Bartonian of Europe and its bearings on the evolution and ecology of massive hyaenodonts (Mammalia). *PLoS ONE* 10(10):e0141941. <https://doi.org/10.1371/journal.pone.0135698>

- Solé, F., Essid, E.M., Marzougui, W., Temani, R., Ammar, H.K., Mahboubi, M., Marivaux, L., Vianey-Liaud, M., and Tabuce, R. 2016. New fossils of Hyaenodonta (Mammalia) from the Eocene localities of Chambi (Tunisia) and Bir el Ater (Algeria), and the evolution of the earliest African hyaenodonts. *Palaeontologia Electronica*, 19.3.41A:1-23. <https://doi.org/10.26879/598>
 palaeo-electronica.org/content/2016/1598-new-eocene-african-hyaenodonts
- Solé, F., Gheerbrant, E., and Godinot, M. 2011. New data on the Oxyaenidae from the Early Eocene of Europe; biostratigraphic, paleobiogeographic and paleoecologic implications. *Palaeontologia Electronica*, 14.2.13A:1-41. palaeo-electronica.org/2011_2/258/index.html
- Solé, F., Lhuillier, J., Adaci, M., Bensalah, M., Mahboubi, M., and Tabuce, R. 2014. The hyaenodontidans from the Gour Lazib area (?early Eocene, Algeria): implications concerning the systematics and the origin of the Hyainailourinae and Teratodontinae. *Journal of Systematic Paleontology*, 12:303-322. <https://doi.org/10.1080/14772019.2013.795196>
- Spaulding, M., O'Leary, M.A., and Gatesy, J. 2009. Relationships of Cetacea (Artiodactyla) among mammals: increased taxon sampling alters interpretations of key fossils and character evolution. *PLoS ONE*, 4(9):e7062. <https://doi.org/10.1371/journal.pone.0007062>
- Stern, J.T. and Susman, R.L. 1983. The locomotor anatomy of *Australopithecus afarensis*. *American Journal of Physical Anthropology*, 60:279-317. <https://doi.org/10.1002/ajpa.1330600302>
- Szalay, F.S. 1967. The affinities of *Apterodon* (Mammalia, Deltatheridia, Hyaenodontidae). *American Museum Novitates*, 2293:1-17. <http://hdl.handle.net/2246/3088>
- Townsend, G., Bockmann, M., Hughes, T., and Brook, A. 2012. Genetic, environmental and epigenetic influences on variation in human tooth number, size and shape. *Odontology*, 100:1-9. <https://doi.org/10.1007/s10266-011-0052-z>
- Tseng, Z.J., Grohé, C., and Flynn, J.J. 2016. A unique feeding strategy of the extinct mammal *Koloponomus*: convergence on sabretooths and sea otters. *Proceedings of the Royal Society B*, 283(1826). <https://doi.org/10.1098/rspb.2016.0044>
- Turner, A.H., Pritchard, A.C., and Matzke, N.J. 2017. Empirical and Bayesian approaches to fossil-only divergence times: a study across three reptile clades. *PLOS ONE*, 12(2):e0169885. <https://doi.org/10.1371/journal.pone.0169885>
- Uhen, M.D. 2000. Replacement of deciduous first premolars and dental eruption in archaeocete whales. *Journal of Mammalogy*, 81:123-133. [https://doi.org/10.1644/1545-1542\(2000\)081<0123:RODFPA>2.0.CO;2](https://doi.org/10.1644/1545-1542(2000)081<0123:RODFPA>2.0.CO;2)
- Urduy, S., Wilson, L.A.B. Haug, J.T., and Sánchez-Villagra, M.R. 2013. On the unique perspective of paleontology in the study of developmental evolution and biases. *Biological Theory*, 8:293. <https://doi.org/10.1007/s13752-013-0115-1>
- Van Valen, L. 1967. New Paleocene insectivores and insectivore classification. *Bulletin of the American Museum of Natural History*, 135:217-284. <http://hdl.handle.net/2246/358>
- Van Valkenburgh, B. 1988. Incidence of tooth breakage among large, predatory mammals. *The American Naturalist*, 131:291-302. <https://doi.org/10.1086/284790>
- Van Valkenburgh, B. 2007. Déjà vu: the evolution of feeding morphologies in the Carnivora. *Integrative and Comparative Biology*, 47:147-163. <https://doi.org/10.1093/icb/icm016>
- Veitschegger, K. and Sánchez-Villagra, M.R. 2016. Tooth eruption sequences in cervids and the effect of morphology, life history, and phylogeny. *Journal of Mammalian Evolution*, 23:251-263. <https://doi.org/10.1007/s10914-015-9315-8>
- White, P.A. and Belant, J.L. 2016. Individual variation in dental characteristics for estimating age of African lions. *Wildlife Biology*, 22:71-77. <https://doi.org/10.2981/wlb.00180>
- Zack, S.P. 2011. New species of the rare early Eocene creodont *Galecyon* and the radiation of the early Hyaenodontidae. *Journal of Paleontology*, 85:315-336. <https://doi.org/10.1666/10-093.1>
- Zack, S.P. 2012. Deciduous dentition of *Didymictis* (Carnivoramorpha: Viverravidae): implications for the first appearance of "Creodonta." *Journal of Mammalogy*. 93:808-817. <https://doi.org/10.1644/11-MAMM-A-245.1>

APPENDIX 1.

Character-taxon matrix used in this study, formatted for the program Mesquite (mesquiteproject.org). See palaeo-electronica.org/content/2017/2056-deciduous-hyaenodont-teeth for zipped file of appendix PDFs.

APPENDIX 2.

Descriptions of the characters used in this analysis with the source of the character or comparable characters from other analyses. See palaeo-electronica.org/content/2017/2056-deciduous-hyaenodont-teeth for zipped file of appendix PDFs.

APPENDIX 3.

List of all the taxa and specimens used in this analysis, along with information on age and locality data. See palaeo-electronica.org/content/2017/2056-deciduous-hyaenodont-teeth for zipped file of appendix PDFs.

APPENDIX 4.

Input file for the Bayesian phylogenetic analysis, formatted for MrBayes (mrbayes.sourceforge.net). See palaeo-electronica.org/content/2017/2056-deciduous-hyaenodont-teeth for zipped file of appendix PDFs.

APPENDIX 5.

Consensus “allcompat” (majority-rule plus compatible groups) tree from Bayesian phylogenetic analysis. See palaeo-electronica.org/content/2017/2056-deciduous-hyaenodont-teeth for zipped file of appendix PDFs.